Final Report for "Glacier and perennial snowfield mass balance of Rocky Mountain National Park (ROMO): Past, Present, and Future"

Task Agreement Number P16AC00826

PI Dr. Daniel McGrath
June 28, 2019
Department of Geosciences
Colorado State University
Daniel.mcgrath@colostate.edu

Andrews Glacier in August 2016

Tyndall Glacier LiDAR scan in May 2016

Summary of Key Project Outcomes

- Over the past ~50 years, geodetic glacier mass balances for four glaciers along the Front Range have been highly variable; for example, Tyndall Glacier thickened slightly, while Arapaho Glacier thinned by >20 m. These glaciers are closely located in space (~30 km) and hence the regional climate forcing is comparable. This variability points to the important role of local topographic/climatological controls (such as wind-blown snow redistribution and topographic shading) on the mass balance of these very small glaciers (~0.1-0.2 km^2).

- Since 2001, glacier area (for 11 glaciers on the Front Range) has varied ± 40%, with changes most commonly driven by interannual variability in seasonal snow. However, between 2001 and 2017, the glaciers exhibited limited net change in area. Previous work (Hoffman et al., 2007) found that glacier area had started to decline starting in ~2000.

- Seasonal mass turnover is very high for Andrews and Tyndall glaciers. On average, the glaciers gain and lose ~9 m of elevation each year. Such extraordinary amounts of snow accumulation is primarily the result of wind-blown snow redistribution into these basins (and to a certain degree, avalanching at Tyndall Glacier) and exceeds observed peak snow water equivalent at a nearby SNOTEL station by 5.5 times.

- Ground-penetrating radar surveys of Andrews Glacier revealed that portions of the glacier exceed 45 m in thickness, likely making this the thickest glacier in Colorado.

- In the upper reaches of Andrews Creek, between 50-75% of the streamflow in the late summer is likely sourced from glacial meltwater.

- Streams fed by glacial meltwater have temperatures between 1 and 5 ° C, although lakes (e.g., Emerald Lake or The Loch) within these drainages result in significant warming. The loss of glaciers/perennial ice patches could result in significant changes to downstream ecosystems that are dependent on this cold water input.

Introduction and Background

Small alpine glaciers and perennial snowfields are intrinsically connected to both their immediate alpine and broader downstream ecosystems through the physical and chemical characteristics of the runoff delivered to them. Glacier derived runoff provides crucial water resources in certain regions (Immerzeel et al., 2013), modifies ocean currents (Royer and Grosch, 2006), influences biogeochemical cycling of nutrients, organic matter and contaminants (Anesio and Laybourn-Parry, 2012), and impacts freshwater ecology far downstream (Jacobsen et al., 2012). Moreover, glaciers are iconic features of

mountain landscapes, representing an important tourist attraction and their loss can reduce park visitations (O'Neel et al., 2014).

In general, glacierized catchments modulate typical non-glacierized annual hydrographs by shifting peak flows later in the summer and producing higher specific discharge (Fountain and Tangborn, 1986; Jansson et al., 2003; O'Neel et al., 2014). This influence can be significant even when glacierized area accounts for <5% of the basin, as the resultant discharge pattern reflects the surface energy balance (i.e., snow and ice melt) rather than precipitation (Jansson et al., 2003; Moore et al., 2009). Glacier-derived runoff also has a unique geochemical signature, and thus, changes in the relative contribution of this runoff can modify downstream environments (Baron et al., 2009; Hood et al., 2015).

Peak snow water equivalents (SWE) and runoff peaks have shifted earlier in the mountains of the western United States in recent decades due to increase rain-snow fraction and warmer spring temperatures (Stewert et al., 2004; Knowles et al., 2006; Mote et al., 2006) producing a significant stress on these alpine ecosystems (van Mantgem et al., 2009). Glaciers may initially help moderate this environmental stress through increased runoff production (Kaser et al., 2010), although as this comes as a deficit to glacial mass, it can, if sustained for years to decades, deplete the reservoir (Jansson et al., 2003).

Glaciers are sensitive indicators of climate change, responding on annual to decadal time scales to changes in climate forcings (i.e., temperature and precipitation). Globally, glaciers have been retreating from highstands at the end of the Little Ice Age (circa 1880), although rates have accelerated rapidly in the past two decades due to anthropogenic forced warming (Marzeion et al., 2014), producing a significant contribution to global sea level rise (Zemp et al., 2019). In the short-term, glacier mass loss can lead to increased runoff, although as glacierized area retreats over the long-term, runoff will dwindle (Immerzeel et al., 2013; Bliss et al., 2014).

Rocky Mountain National Park (ROMO) contains ~30 perennial ice patches/glacierets, ranging in size from 0.006 to 0.13 sq. km[1], which are predominantly found in north- to east- facing high elevation cirques (Hoffman et al., 2007). Seven of these features (Andrews, Mills, Moomaw, Rowe, Sprague, Taylor and Tyndall) are labeled as "glaciers" on the USGS topographic map, although as this report details, only Andrews Glacier exhibits characteristics consistent with being classified as a glacier or glacieret (Lliboutry, 1965). The primary distinction between a glacier and an ice patch is the presence of internal motion or deformation (Serrano et al., 2011), which requires ~30 m of ice. Throughout this report, the term glacier and glacieret will be used interchangeably and these named features will be referred to as glaciers (primarily because historical precedence), despite evidence suggesting that they no longer actively deform.

[1] In the analysis presented here, the largest feature in ROMO is Icefield snowfield at ~0.084 sq. km in 2017.

These glaciers are found below the regional equilibrium line altitude. Previous work has shown that they are sustained by extremely high rates of preferential snow accumulation due to both wind redeposition (4- 8 times regional accumulation) and avalanching, and reduced ablation through topographic shading (Outcalt and MacPhail, 1965; Hoffman et al., 2007; Moore et al., 2009). Although less common in ROMO, debris cover can play an important role in decoupling small glaciers from the regional climate, with Teton Glacier in Grand Teton National Park being an excellent example.

Interannual net mass balance variability is typically large for these glaciers and glacier size/elevation ranges are relatively small, which produces the unusual situation where the entire glacier is either entirely in the accumulation or ablation zone (in contrast to most glaciers, which have distinct zones on the glacier, separated by the equilibrium line). Previous work suggested that this variability was predominantly tied to the summer energy balance (strongly correlated to air temperatures), and less dependent on winter snow accumulation variability, as direct snowfall is a minor component of the mass balance regime (Hoffman et al., 2007; Moore et al., 2009).

Research Objectives

This multi-faceted research project sought to develop a process-based understanding of modern glacier mass balance in Rocky Mountain National Park. This understanding was developed in the context of historic glacier response and is used to make informed predictions of future change for improved science-based resource management.

Specific research objectives included:

- Develop a broad process-based understanding of modern glacier mass balance in ROMO
- Leverage historical climate data and photo archives to yield an improved understanding of historic glacier response
- Make informed predictions of future change based on downscaled climate model projections and process understanding developed in the study

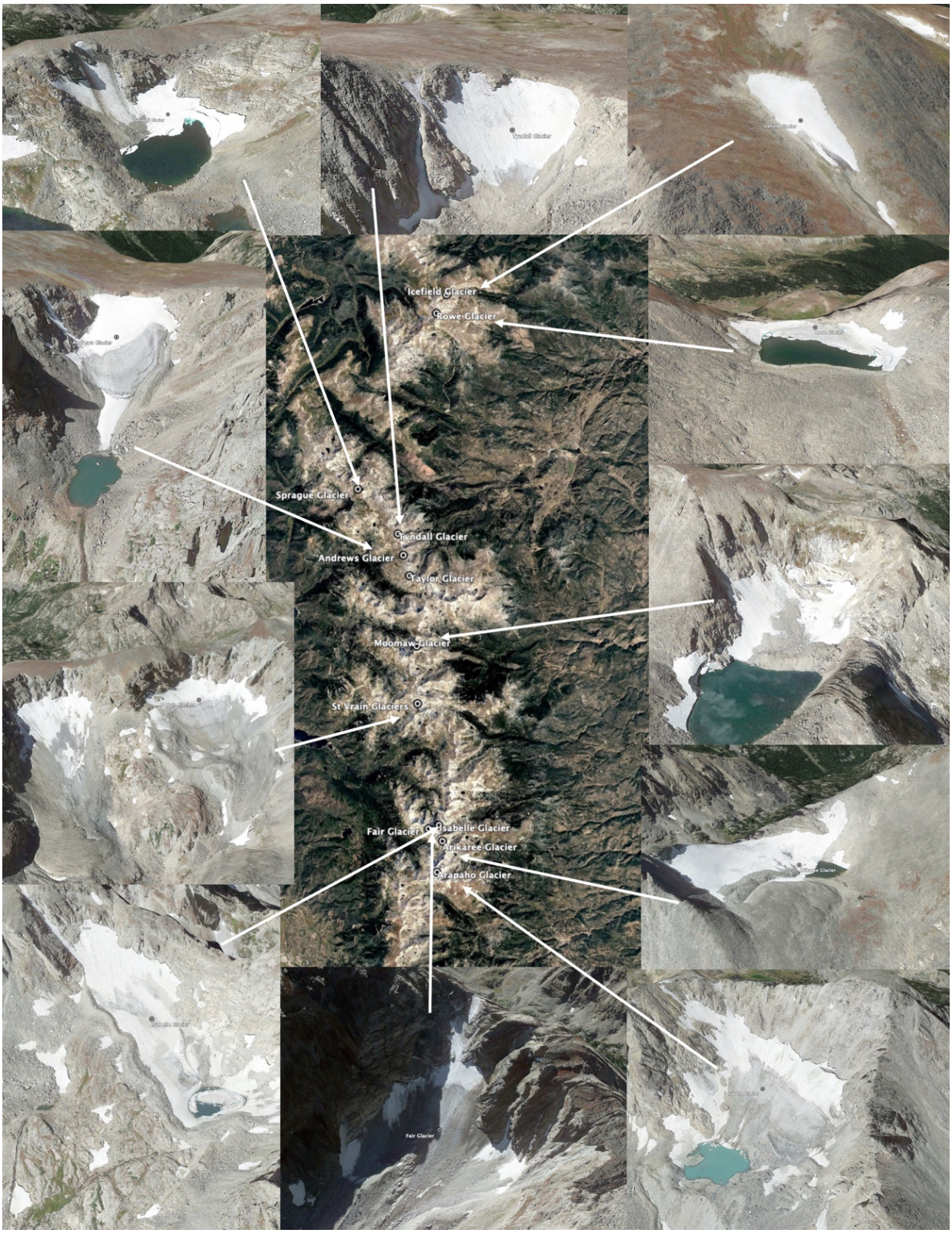

Figure 1. Key glacierets/perennial ice patches studied along Colorado's Front Range, including six features in ROMO: Icefield, Rowe, Sprague, Tyndall, Andrews and Moomaw glaciers.

Section 1. Decadal Scale Glacier Area Change and Drivers

Previous work by Hoffman et al. (2007) documented glacier area change over the past ~100 years for the many perennial ice patches/glacierets in ROMO. This work found that glaciers retreated from ~1900 to ~1940, expanded to the end of the century, at which point they noted that glacier area had started to decline. This progression can clearly be seen in historic photographs of Andrews Glacier (Figure 2) and in the Hoffman et al. (2007) timeseries (Figure 3). Of note, is that glacier area (and qualitatively, glacier volume) was smaller in 1940 than at present (see talus emerging near the terminus of Andrews Glacier in 1940). Photographs of Tyndall Glacier from 1940 suggest this glacier was comparable in size (or perhaps smaller) to present. The images below also illustrate that glacier volume can change rapidly (on the order of decades), as can be seen from 1916 to 1940.

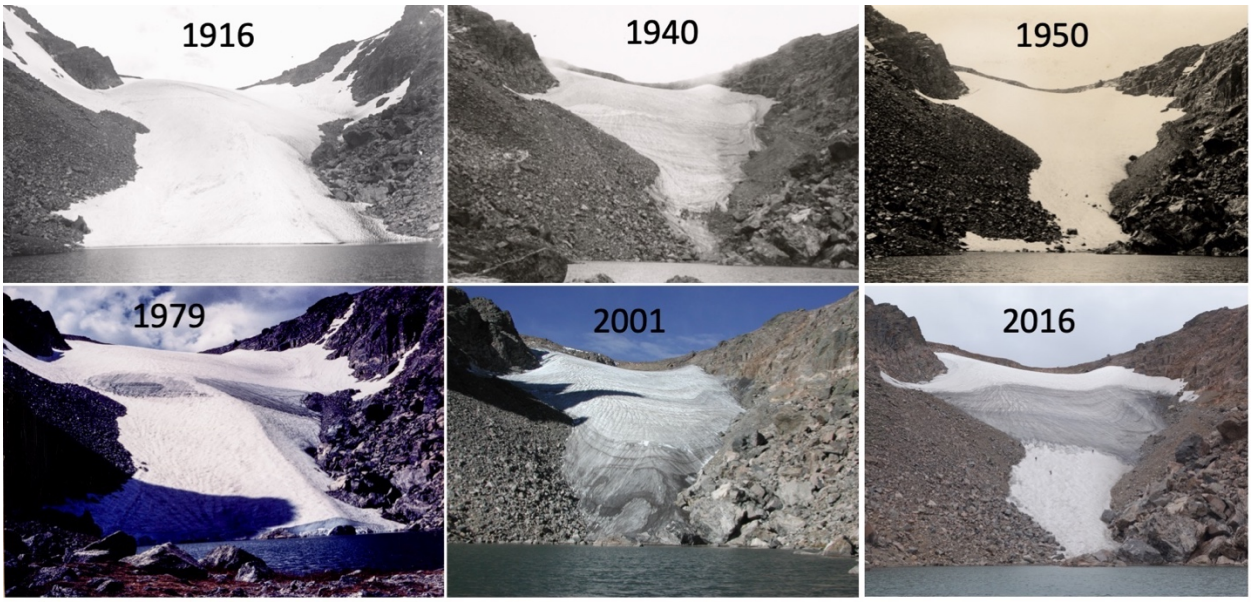

Figure 2. Photographic timeseries of Andrews Glacier. Photo credits: 1916: Lee Willis/NSIDC; 1940: Paul Nesbit/NSIDC; 1950: ROMO Glacier Report/NSIDC; 1979: Russell Allen/NSIDC; 2001: unknown/Rocky Mountain National Park Library; 2016: Daniel McGrath

As part of this project, glacier area timeseries were established for 11 glaciers along the Front Range using imagery primarily sourced from the National Agricultural Imagery Program (NAIP; https://www.fsa.usda.gov/programs-and-services/aerial-photography/imagery-programs/naip-imagery/). NAIP imagery is currently collected in late summer at two year intervals (in Colorado), has three spectral bands, and 1-meter ground sample distance. This imagery was downloaded from the USGS EarthExplorer data portal (earthexplorer.usgs.gov).

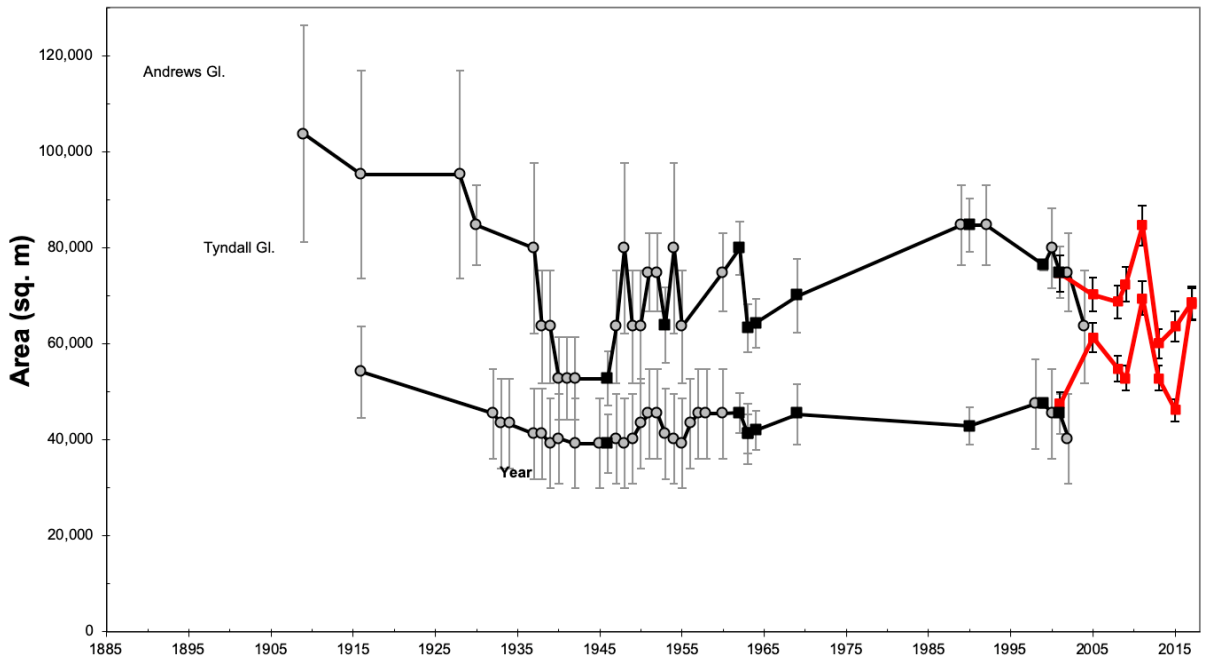

Figure 3. Change in area of Andrews and Tyndall glaciers (adapted from Hoffman et al., 2007). Glacier areas measured by this project are shown in red.

A notable finding of this project is that the decline in glacier area starting ~2000, as noted by Hoffman et al. (2007), was not sustained in the 21st century. Glacier area was found to be stable at Andrews and slightly increasing at Tyndall over the past ~15 years, but with high interannual variability, likely reflecting significant variability in seasonal snow accumulation. This variability in snow accumulation is clearly shown in peak/maximum snow water equivalent (SWE) measurements at the Bear Lake and Niwot SNOTEL sites (Figure 4), which exhibited two to three-fold variability over this period.

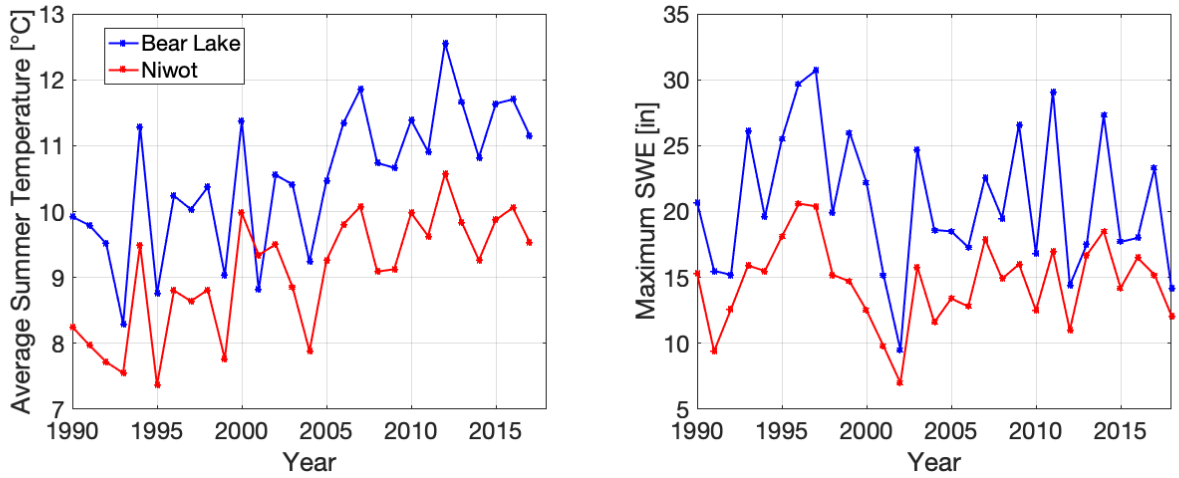

Figure 4. Average summer temperature and maximum/peak SWE at the Bear Lake and Niwot SNOTEL sites from 1990-2017).

As noted above, the glacier area analysis was expanded to include 11 glaciers along the Front Range, including six glaciers/ice patches in ROMO (Andrews, Icefield, Moomaw, Rowe, Sprague and Tyndall). These 11 glaciers show a consistent picture of high interannual variability but limited net change over this 16 year interval. Of particular note was the ~80% change in glacier area between 2011 and 2012, which reflects the 100% change in peak SWE measured at Bear Lake SNOTEL (Figure 4). Over this period, glacier areas remained stable or slightly increased despite warming summer air temperatures (Figure 4; Fassnacht et al., 2018). Considering the longer timeseries compiled by Hoffman et al. (2007), Tyndall and Andrews glaciers have comparable or slightly larger areas than in the 1960s, which stands in stark contrast to glaciers in both the Wind River Range and Teton Range that have decreased in area by 39 and 25% between 1966/67 and 2006, respectively (Maloof et al., 2014; Edmunds et al., 2012).

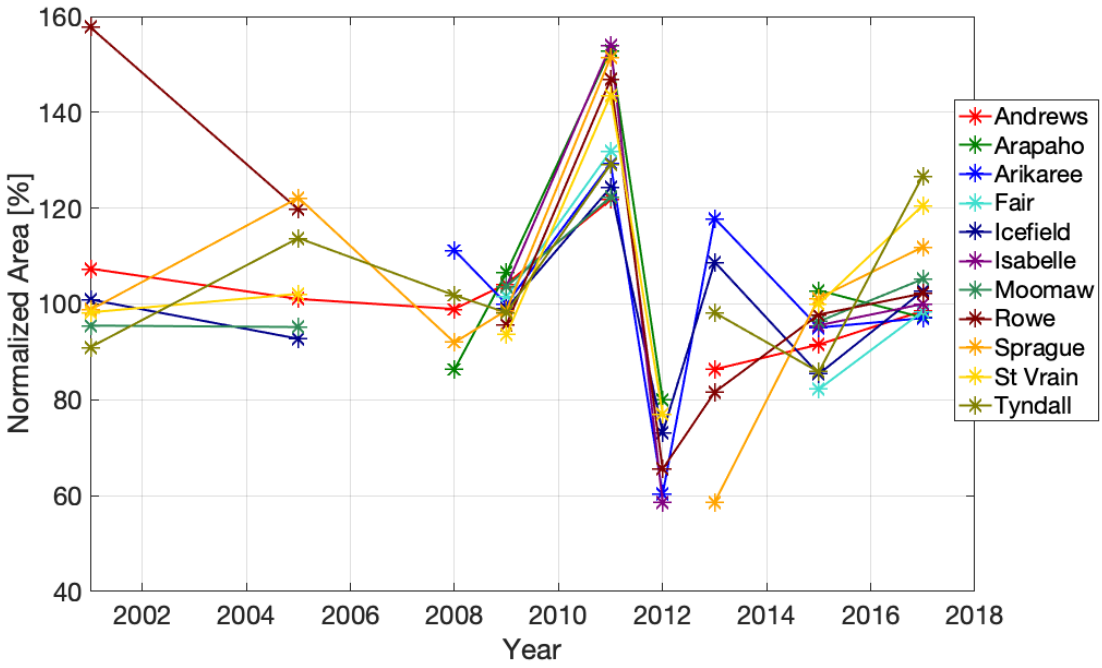

Figure 5. Normalized area (area/mean area over interval) time series for 11 glaciers along the Front Range. However, there is limited net change over this interval, which is unique in comparison to other published work looking at glacier change in the contiguous US, which typically report significant glacier retreat.

In order to quantify the relative importance of winter accumulation and summer temperature variability in controlling glacier area, area change anomalies were regressed against summer temperature and winter snow anomalies derived from local SNOTEL sites (Bear Lake, site #322 and Niwot, site # 663). The summer temperature and winter snow anomalies were weighted from 0 to 100% in the least

squares regressions and the coefficients of determination from these regressions were assessed as a metric of the relative importance of each term (Figure 6). For Arikaree, Fair, Isabelle and Moomaw glaciers, winter snow accumulation variability exhibited a strong control on glacier area variability. For Andrews and Rowe glaciers, summer temperatures were found to exert a greater control on area variability. Lastly, for Arapaho, Sprague, St. Vrain and Tyndall glaciers, the coefficients of determination were lower, but all showed winter accumulation variability to be more important.

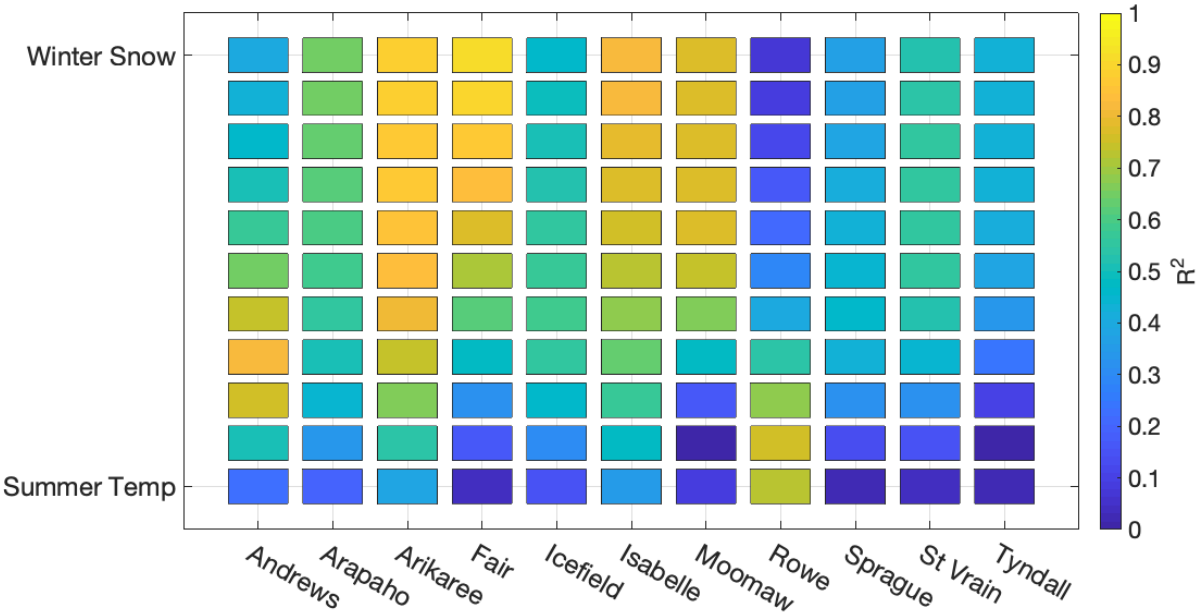

Figure 6. Correlation between summer temperature and winter accumulation anomalies (derived from nearby SNOTEL site) and glacier area change.

This analysis points to winter accumulation variability playing an important role in controlling glacier area variability for most of these glaciers. However, this is not uniform across all glaciers, which suggests that a combination of topographic/morphological and/or local climatological factors strongly, and uniquely, influence their mass balance regimes. To better understand these secondary factors, two additional metrics were derived: upwind surface elevation profiles and normalized solar radiation forcings. Although almost all of these glaciers are found in high-elevation, east to northeast facing cirques that see both preferential wind-blown snow redistribution and topographic shading, these parameters are clearly not equal across all sites. The first parameter, which is related to the potential for wind-blown snow redistribution, is calculated as the percentage of topography within 1500 m of each glacier's centroid in the upwind direction (WSW) that is within 100 m relief of the local ridge top elevation (Figure 7). Four glaciers, Andrews, Icefield, Sprague, and Tyndall, have 40% (600 m; profiles shown with thickened line widths) or more topography within 100 m of the local ridge top elevation, making these

glaciers/basins particularly disposed to wind-blown snow redistribution. This difference can also be seen in Figure 8, which shows oblique 3-D views of Tyndall and Arapaho glaciers. For Tyndall, the high-elevation peneplain extends more than 1000 m to the west, while to the west of Arapaho, there is only a sharp ridgeline (Figure 8). This high-elevation peneplain plays as essential role in the seasonal mass balance of Tyndall (and Andrews) Glacier, as this feature is scoured all winter and the snow is redistributed onto the glacier.

The second parameter, a measure of topographic shading, was calculated in ArcMap 10.5 using the Solar Radiation toolbox. Average shortwave radiation values were calculated over the June-August period and then subsequently normalized by the maximum value in the study area (Figure 9).

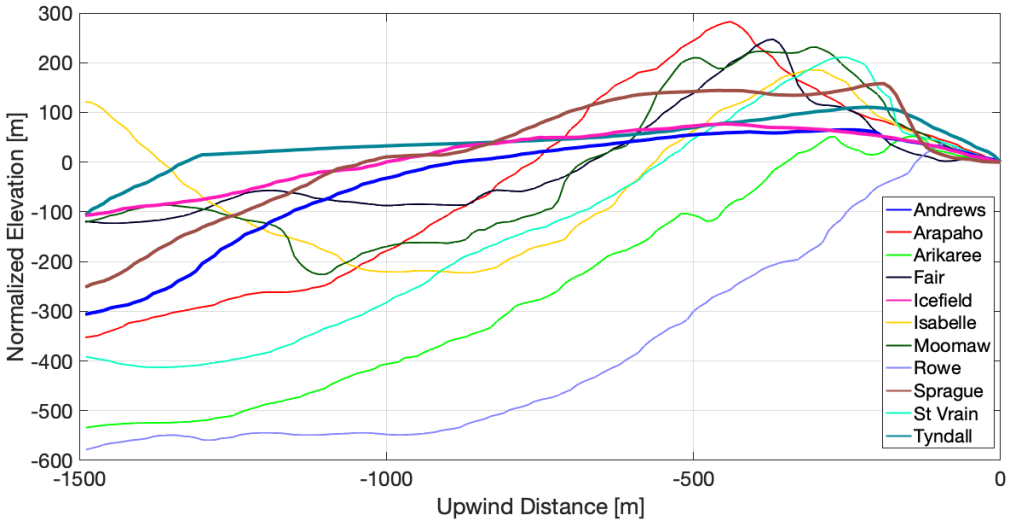

Figure 7. Normalized surface elevations along a 1500 m profile in the upwind direction from each glacier's centroid. Glaciers where 40% or more of the topography within the first 1500 m is within 100 m of the local ridge top elevation are shown in bold and are preferentially located to see wind-blown snow redistribution.

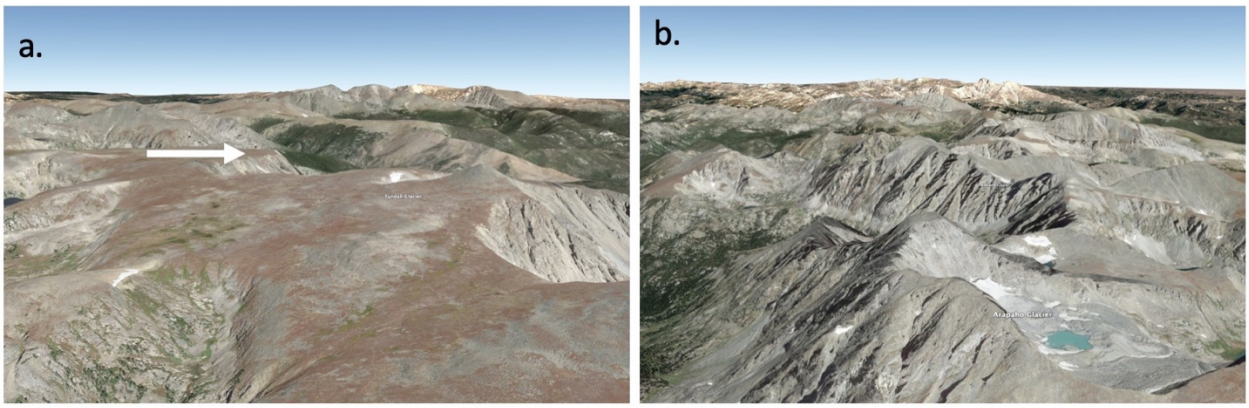

Figure 8. Oblique views of Tyndall (a) and Arapaho (b) glaciers in Google Earth. Both images are looking north and the mean wind direction is left to right.

Significant differences in solar forcing are also observed across these 11 glaciers. For instance, Fair Glacier (the only glacier with a westerly aspect) sees only ~50% normalized incoming solar radiation, while Rowe Glacier sees nearly 90% of the maximum incoming solar radiation. Such differences likely explain the differences shown in Figure 6, where Rowe is much more sensitive to summer temperatures, while Fair is much more sensitive to snow accumulation variability.

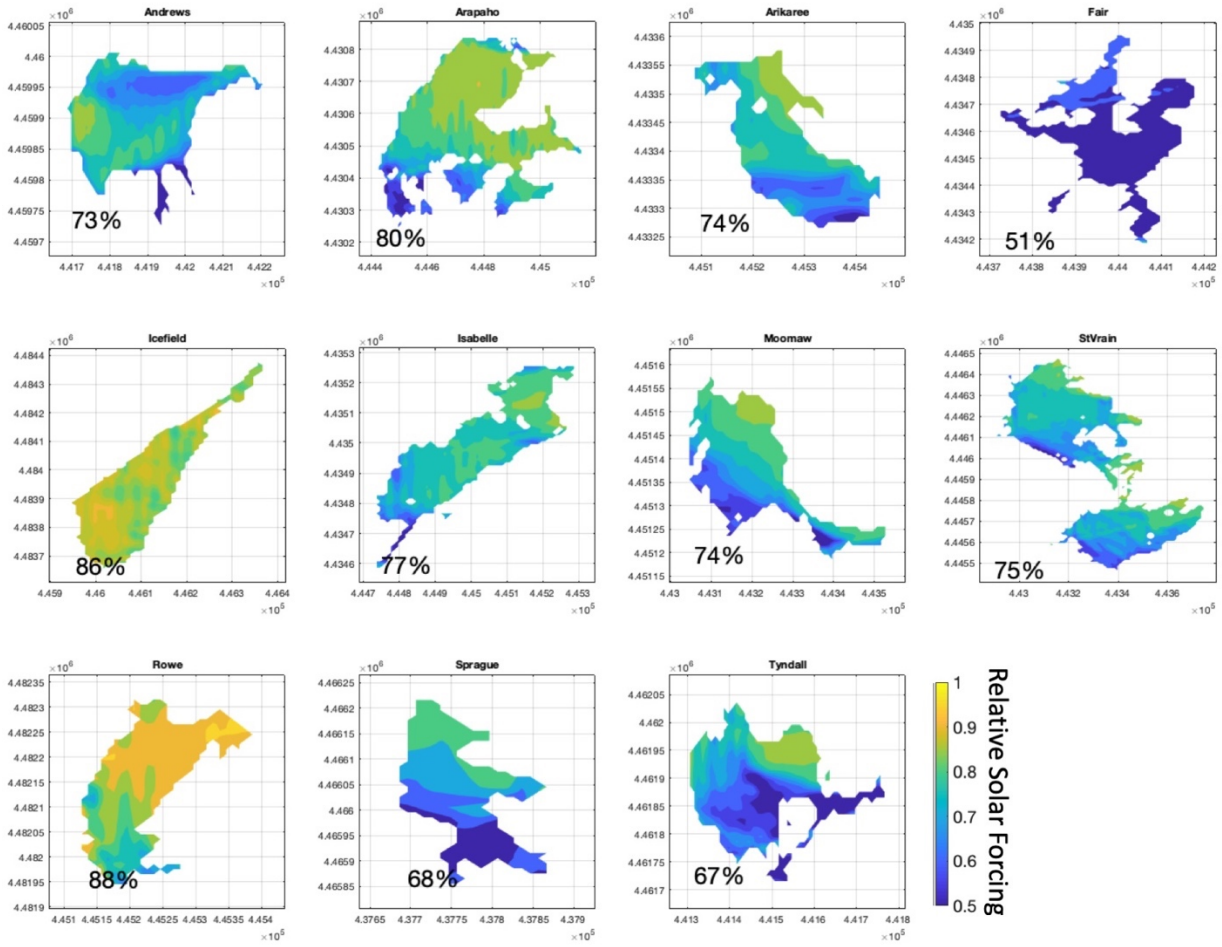

Figure 9. Normalized solar radiation for each of the 11 glaciers. The solar forcing is normalized by the maximum value in the study area and is consistent for all glaciers. Average values for each glacier are reported as percentages in the bottom left of each subpanel.

Previous work by Outcalt and MacPhail (1965), Johnson (1979), and Hoffman et al. (2007) found that glaciers along the Front Range were more sensitive to summer ablation variability, rather than direct winter snow accumulation variability, as any deficits in the latter were overcome by wind re-distribution. While this is likely true for Andrews and Rowe glaciers, it does not appear that this is uniformly true for all glaciers along the Front Range, as others, like Fair and Isabelle, which likely see less wind

redistribution than other glaciers, appear to be more sensitive to interannual variability in direct snow accumulation.

Importantly, area, as a metric for characterizing glacier change, is fraught with uncertainty when examining glaciers with areas as small as these glaciers. These glaciers clearly exhibit significant interannual variability in area (Figure 5), although these changes are driven by modest thicknesses of seasonal snow/firn around the fringes, which remain highly sensitive to meteorological forcings the following year. As described in Section 3, this analysis was supplemented with glacier volume change over a ~50 year interval, using photogrammetrically derived topographic maps from 1963/64 and high-resolution DEMs produced from DigitalGlobe Worldview-3 stereo satellite image pairs.

Section 2. Seasonal mass balances of Tyndall and Andrews glaciers

A primary focus of this project was to understand the seasonal and net mass balance of Tyndall and Andrews glaciers. This task was accomplished through repeat terrestrial LiDAR surveys of each glacier in May 2016, September 2016, May 2017 and September 2017. The LiDAR surveys were collected in collaboration with field engineers at UNAVCO, Inc. using a Riegel VZ-4000 scanner. The surveys required one scan location at Tyndall and two scan locations at Andrews. The point clouds were aggregated into 1-m digital elevation models (DEMs) and subsequently differenced from one another to yield seasonal and annual mass balances. In addition to the LiDAR surveys, ground-penetrating radar (GPR) surveys were collected to measure seasonal snow variability on Andrews Glacier. The GPR surveys were conducted with a Mala Geosciences Pro-Ex control unit and a 800 MHz antenna.

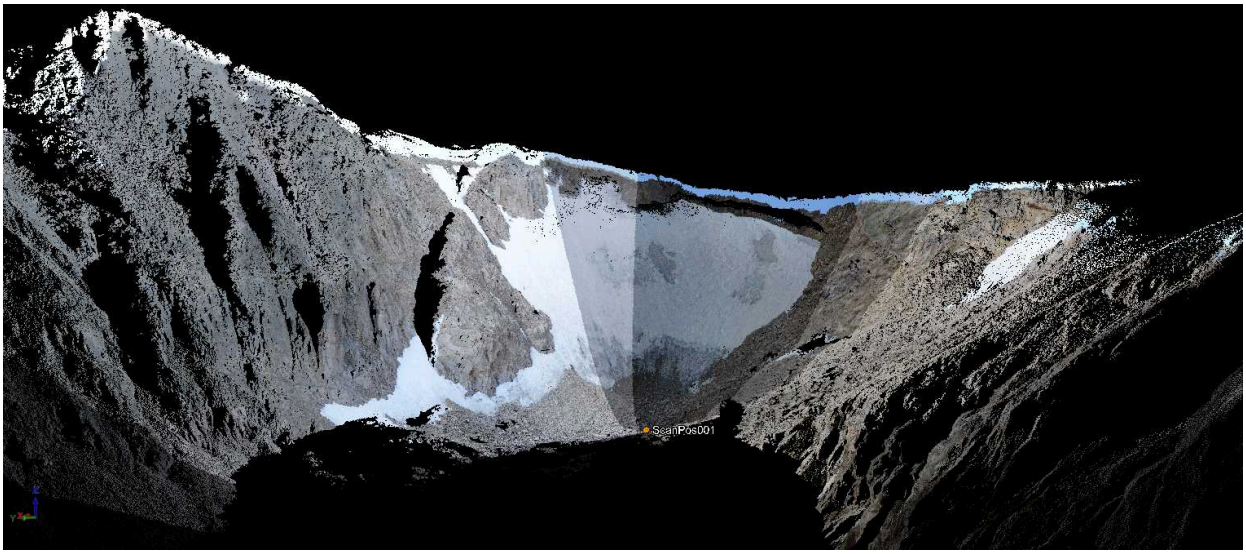

Figure 10. LiDAR point cloud of Tyndall Glacier in September 2016.

Figure 11. Photograph of GPR surveys on Andrews Glacier in May 2016. Photo credit: Rick Aster.

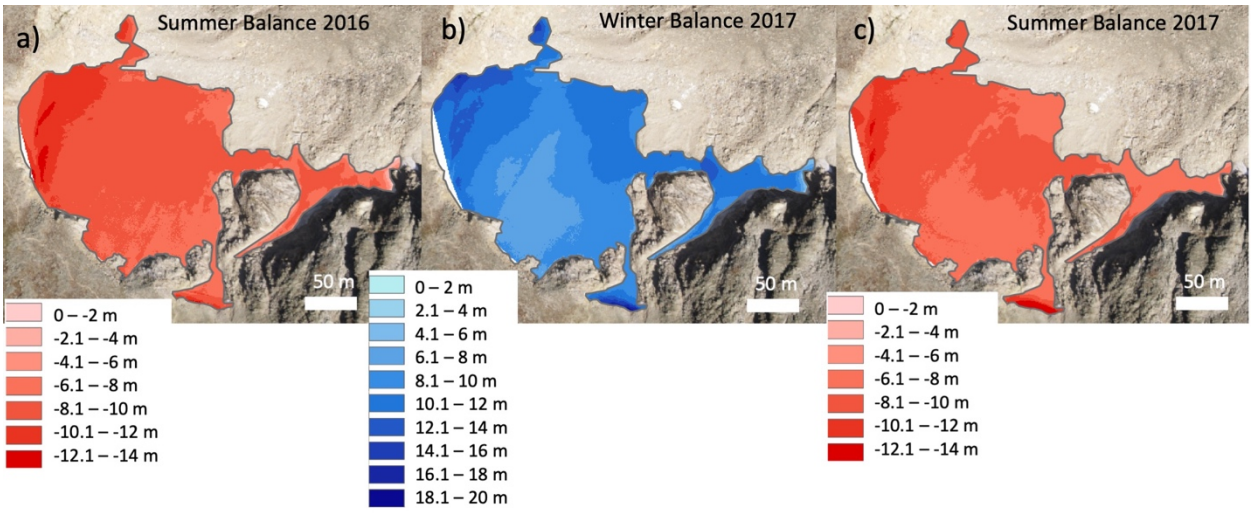

Figure 12. Seasonal elevation differences for Tyndall Glacier.

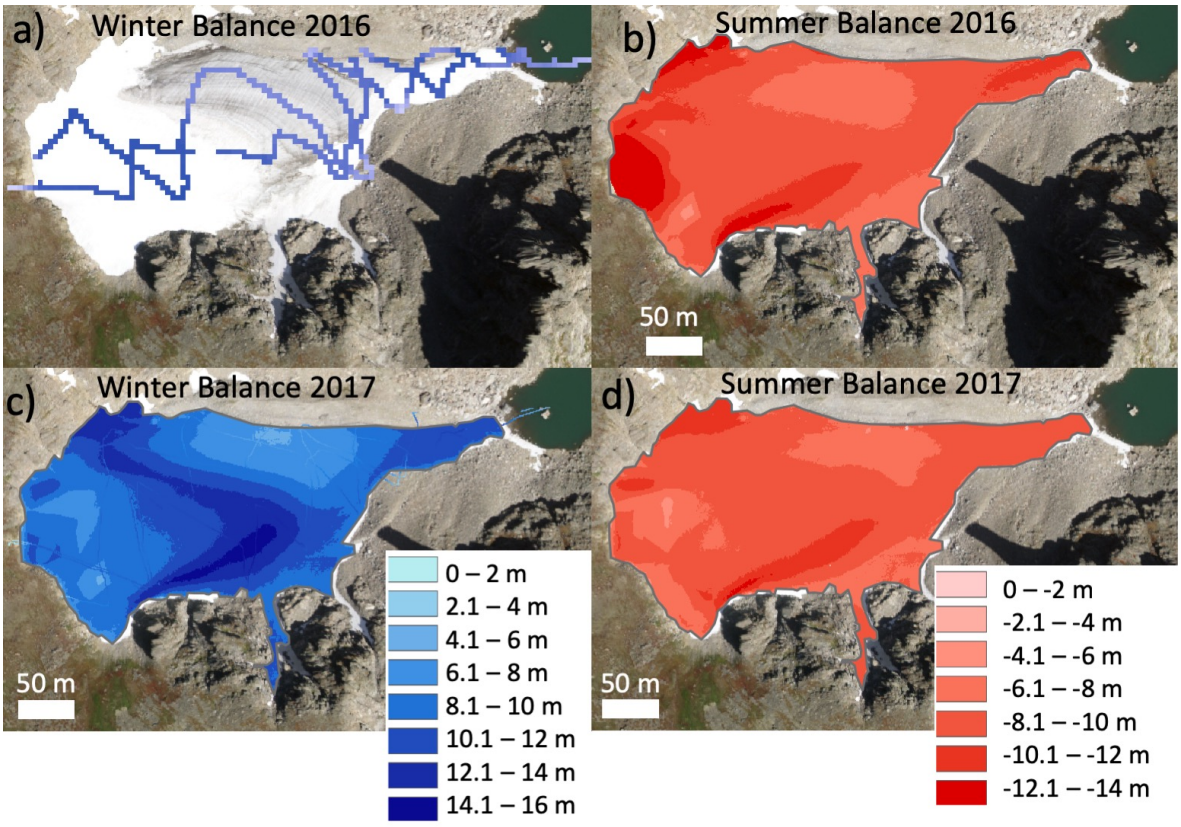

Figure 13. Seasonal elevation differences for Andrews Glacier. The 2016 winter balance was derived from GPR surveys, while subsequent balances were derived from repeat LiDAR surveys. GPR derived snow depths are overlaid on the winter balance 2017 in subpanel c.

Table 1. Seasonal elevation differences for Andrews and Tyndall glaciers. Values reported in each column are mean, maximum and minimum.

	Summer 2016 Mean, Max, Min [m]	Winter 2017 Mean, Max, Min [m]	Summer 2017 Mean, Max, Min [m]	Annual 2017 Mean, Max, Min [m]
Andrews Glacier	-9.3, -2.1, -20.5	9.9, 14.9, 2.6	-8.6, 7.3, -12.8	1.4, 4.7,-3.4
Tyndall Glacier	-8.6, -0.4, -13.3	9.7, 19.5, 0.9	-8.4, -0.9, -19.3	1.5, 5.7, -2.8

Both glaciers exhibit ~9 m of seasonal surface elevation change due to winter accumulation and subsequent summer ablation. Field observations suggests that the majority of this winter accumulation is due to wind-blown snow redistribution at Andrews, and a combination of wind-blow redistribution and avalanching (thereby transporting wind-blown snow to the base/terminus of the glacier) at Tyndall. Assuming a snow density of 340 kg/m^3 (2017 snowpit observations), the winter 2017 mass balance was ~3.3 m w.e. In comparison, the peak SWE observed at the Bear Lake SNOTEL in 2017 was 0.59 m,

meaning that 5.5 times more snow/SWE accumulated on the glaciers compared to direct accumulation at the nearest SNOTEL station (~4 km distant, 700 m elevation difference). The summer surface elevation changes were slightly less during summer 2017 compared to summer 2016.

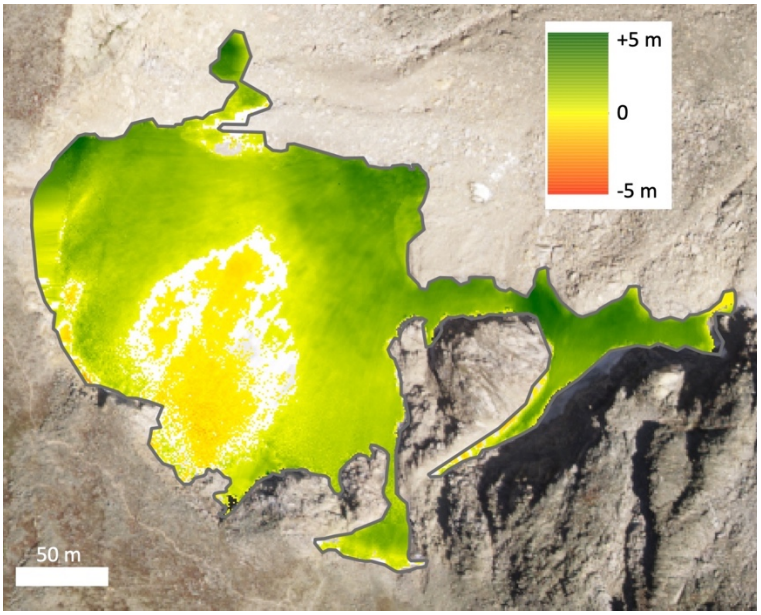

Figure 14. Annual surface elevation change at Tyndall Glacier.

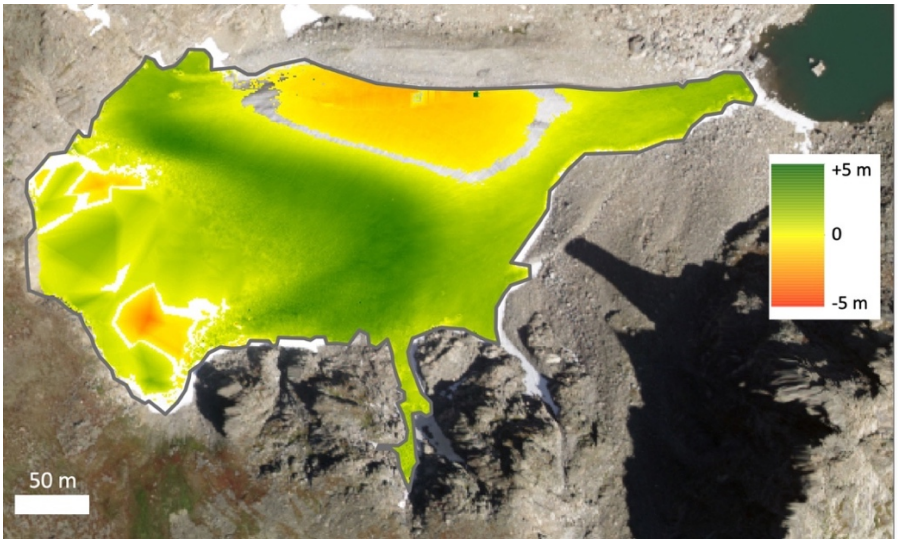

Figure 15. Annual surface elevation change at Andrews Glacier.

Over the two year period, both glaciers saw positive surface elevation changes of 1.4 and 1.5 m, or 0.8 or 0.9 m w.e., assuming a late summer snow density of 600 kg/m^3 (Figures 14 and 15). The surface elevation changes were most positive in locations on each glacier that saw the greatest snow accumulation during the preceding winter, while the annual elevation changes were negative on each glacier where snow

accumulation was at a minimum. These observations suggest that spatial variability in winter accumulation is the dominant control on net (annual) mass balance spatial variability, as summer ablation processes are more uniformly distributed across each glacier's surface.

An additional objective of the GPR surveys was to measure the ice thickness of Andrews Glacier, as this has important implications for the future evolution of this glacier. This survey was conducted with a 250 MHz antenna and resulted in ice thicknesses between ~1 m (most of the lower glacier is <10 m thick) to a maximum of ~47 m, in a central overdeepening at the center of the glacier (Figure 16). GPR surveys of ice thickness on other glaciers along the Front Range are fairly limited, but limited surveys of Arapaho Glacier found maximum ice thicknesses of 15 m (Haugen et al., 2010) and ~25 m on Arikaree Glacier (Leopold et al., 2015). Thus, these findings suggest that Andrews Glacier is the thickest glacier in Colorado and certainly theoretically capable of internal motion/deformation.

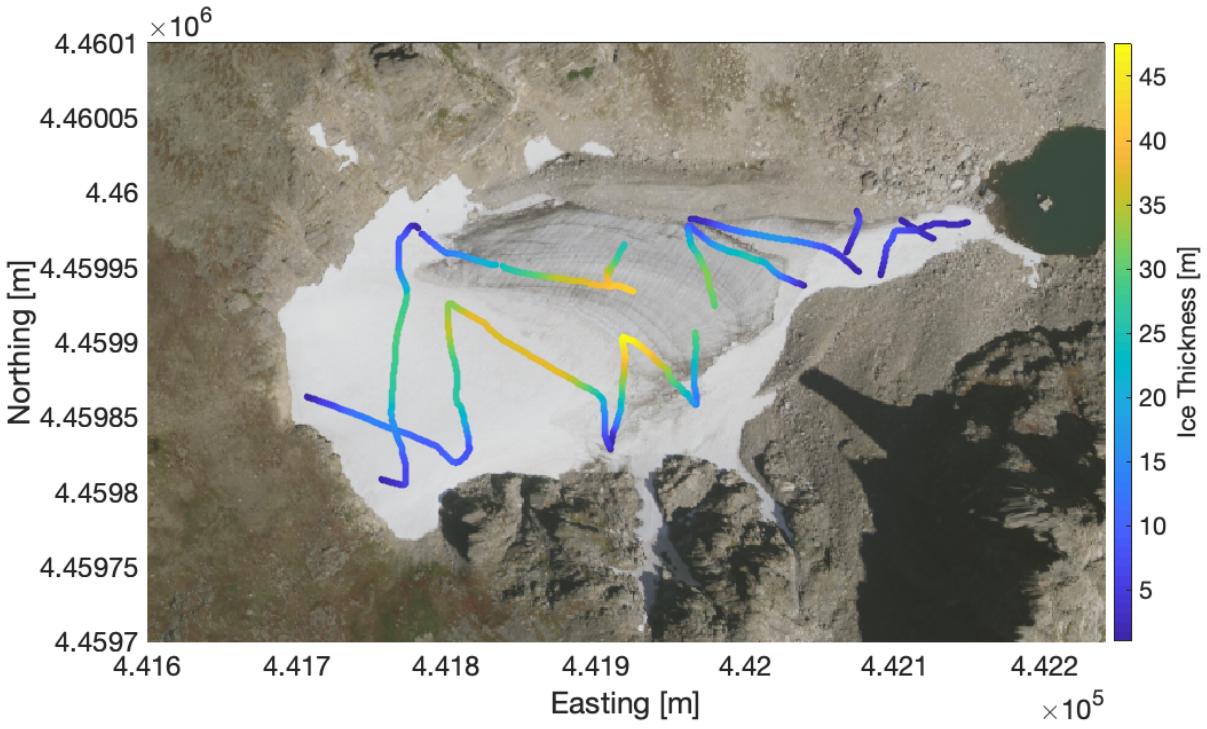

Figure 16. GPR-derived ice thicknesses of Andrews Glacier in May 2017. GPR surveys were conducted using a Mala Geosciences ProEx control unit and 250 MHz antenna.

Section 3. 50-year Geodetic Mass Balance

Glacier volume change was analyzed over an ~50 year interval using photogrammetrically derived topographic maps from 1963/64 (Figure 17) and high-resolution DEMs produced from DigitalGlobe Worldview-3 stereo satellite image pairs.

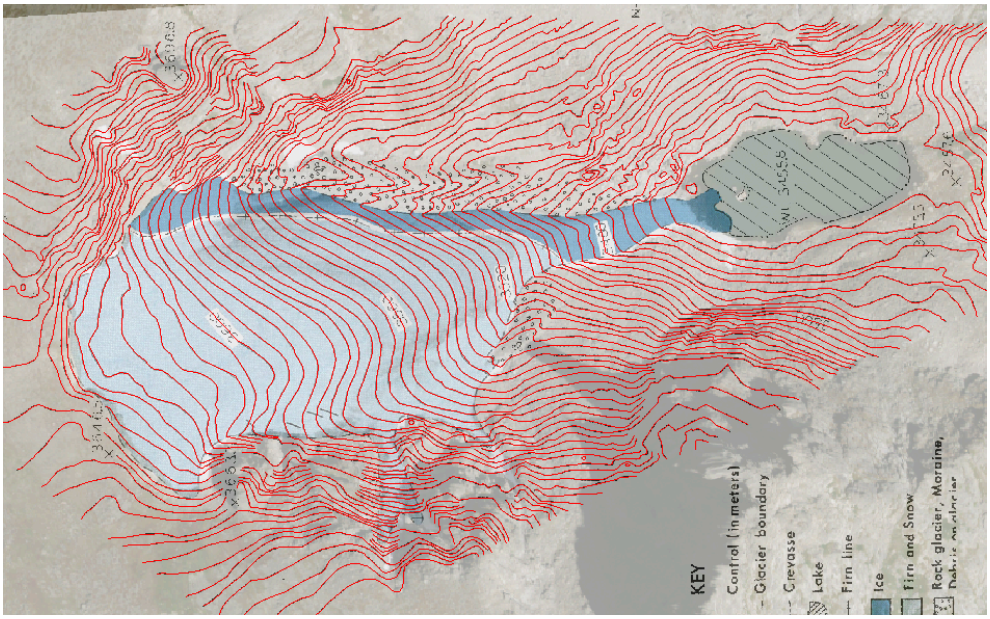

Figure 17. Digitized topographic map of Andrews Glacier, originally produced by Outcalt and MacPhail (1965) using airborne photographs taken in 1963 and 1964.

The original topographic maps were digitally scanned at high-resolution and georeferenced to a modern orthorectified satellite image. Regions of stable ground were subsequently identified (vegetation and snow free; bedrock if possible) and a co-registration method was used (Nuth and Kaab, 2011) that minimized the vertical differences between the historic topographic maps and the modern DEM. The modern DEM was sourced from stereo-image pairs collected on September 7, 2016 from the DigitalGlobe Worldview-3 satellite and processed using SETSM (Mike Willis, personal communication). Once co-registered, the historic topographic map was differenced from the 2016 DEM and the point differences were subsequently kriged across the glacier surface.

Here, results for four glaciers are presented: Arapaho, Moomaw, Andrews and Tyndall glaciers. Arapaho Glacier thinned by -23.3 m on average, resulting in an average change of -0.44 m/yr between 1964 and 2016. The highest rates of change occurred on the northern sections of the glacier, which has a more southerly aspect (Figure 18a). Previous work found average thinning rates of -0.76 m/yr between 1900 and 1960, but only -0.1 m/yr between 1960 and 2005 (Haugen et al., 2010). Andrews Glacier thinned on average by -0.7 m (average change rate of -0.01 m/yr), although this average rate alias distinct spatial patterns. The glacier thickened near the terminus and at the top of the glacier and thinned significantly in the central section (Figure 18d). The airborne/satellite images visually confirm these changes, as the terminus was bare ice in 1963 but snow covered in 2016, while the central section has

extensive snowcover in 1963 and bare ice in 2016 (Figure 18e, f). Tyndall Glacier thickened slightly on average (+1.13 m) between 1964 and 2016, but again, this masks unique spatial patterns of elevation

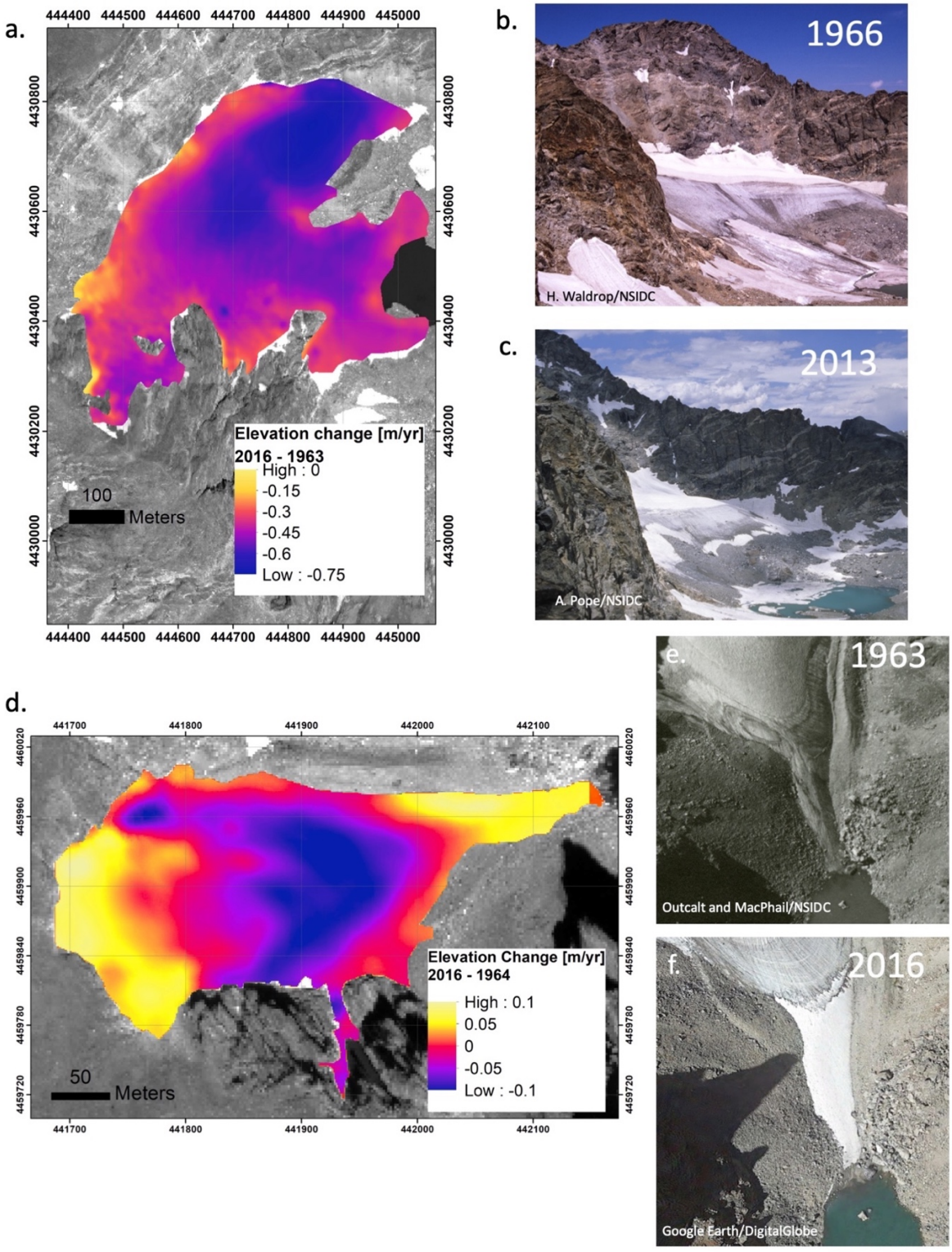

Figure 18. Elevation change for Arapaho and Andrews glaciers.

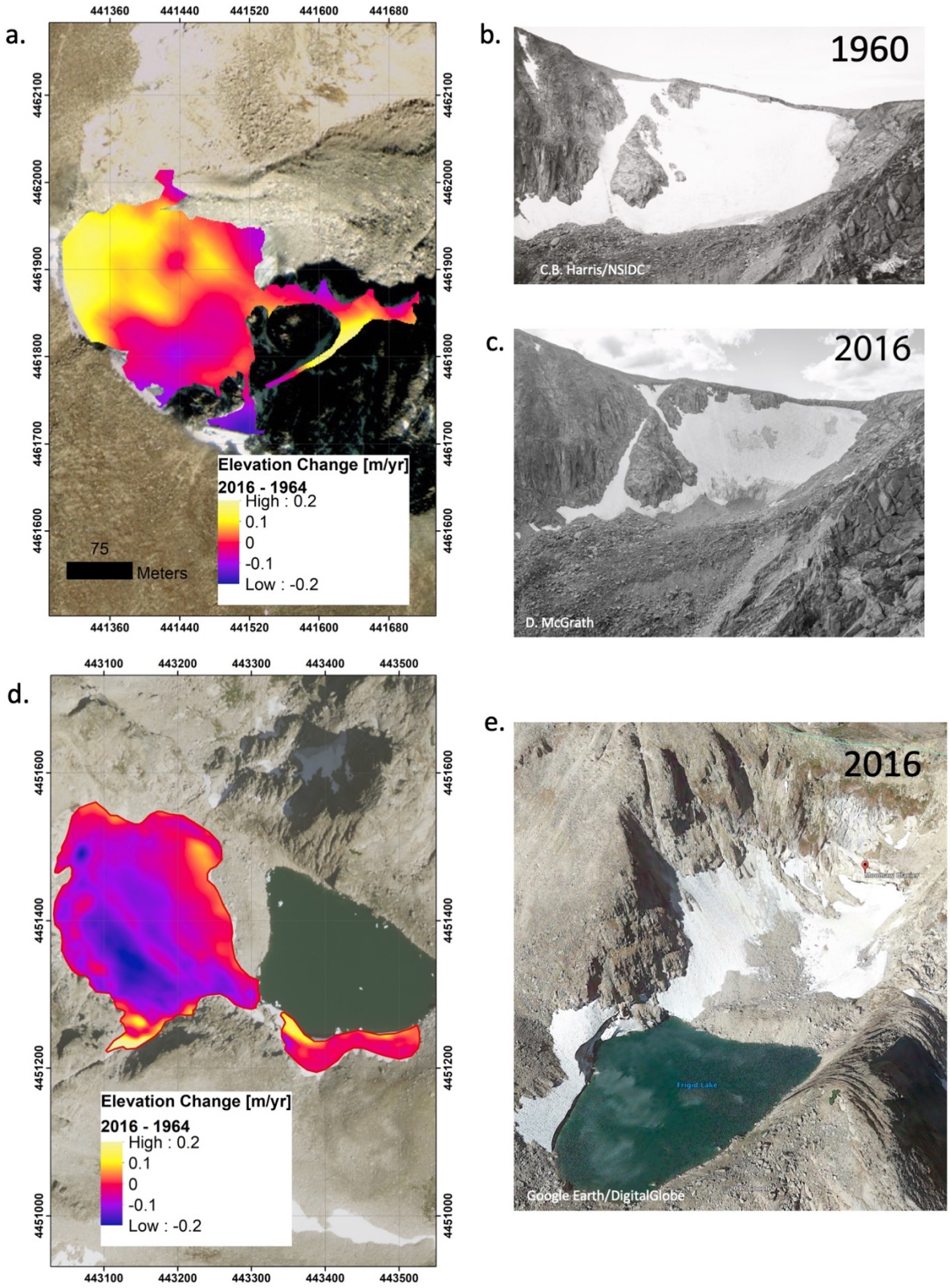

Figure 19. Elevation change for Tyndall and Moomaw glaciers.

change, such that the more easterly aspects thickened and the more northerly aspects of the glacier thinned (Figure 19 a). Lastly, Moomaw Glacier thinned on average by -3.2 m between 1964 and 2016, with a fairly uniform spatial pattern (Figure 19d). By 2016, the Moomaw appears to have largely separated into a few distinct ice patches and the remaining ice appears to be quite thin overall.

Again, one of the more interesting findings of this project has been the distinct differences in mass balance sensitivity – Arapaho Glacier thinned by >20 m, while Tyndall thickened slightly – despite being within ~30 km of one another and experiencing the same regional climate forcings. These differences really emphasize the point that as glaciers/ice patches become increasingly small in size, their mass balance regimes can diverge from regional forcings and respond more significantly to local topographic/morphological and/or local climatological factors. To illustrate this further, average thinning rates for Arapaho and Tyndall glaciers were binned and compared to normalized solar insolation forcings (Figure 20). For Arapaho Glacier, topographic shading plays an important role, as the portions of the glacier that see the least solar energy are closest to equilibrium, whereas the more exposed, southerly aspects of the glacier have thinned by upwards of -0.8 m/year. In contrast, Tyndall Glacier exhibits opposing behavior, such that the sections of the glacier that are most shaded are actually thinning at the greatest rate, hence topographic shading does not appear to be as important of a control at this glacier. However, if we also consider wind-blown snow redistribution, the pattern of elevation change makes more sense – sections of the glacier aligned with the snow redistribution are stable or thickening, while sections that see significantly less snow each winter, are thinning (Figure 12).

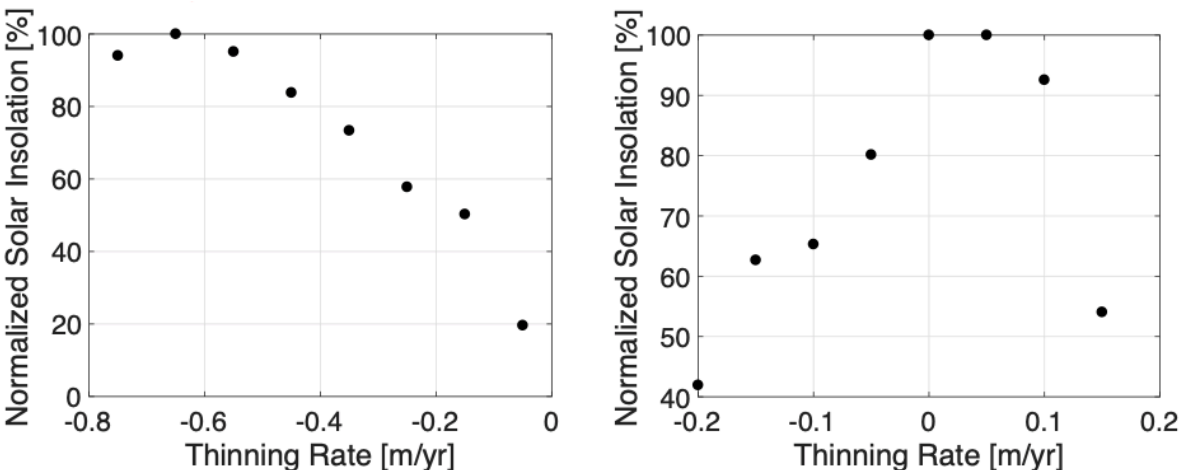

Figure 20. Scatterplots of normalized solar insolation vs thinning rate for Arapaho (left) and Tyndall (right) glaciers.

Section 4. Stream discharge and stream temperatures downstream of ROMO's glaciers

Glacierized catchments typically have distinct hydrologic regimes compared to non-glacierized basins, with later peak flows and higher specific discharge (Fountain and Tangborn, 1986; Jansson et al., 2003; O'Neel et al., 2014). This influence can be significant even when glacierized area accounts for <5% of the basin, as the resultant discharge pattern reflects the surface energy balance (i.e., snow and ice melt) rather than precipitation (Jansson et al., 2003; Moore et al., 2009). Glacier-derived runoff also has a unique geochemical signature, and thus, changes in the relative contribution of this runoff can modify downstream environments (Baron et al., 2009; Hood et al., 2015). The objective of this component of the project was to quantify the hydrologic characteristics of streams draining Andrews and Tyndall glaciers, such that we could contribute to the question: How do glaciers and perennial snowfields modify the hydrology of alpine basins and what are the ecosystem implications of their potential demise?

As part of this work, stream stage gages (capacitance rods) were installed and maintained in Andrews Creek above Andrews Meadow (site name M5; Figure 21) and Tyndall Creek below Emerald Lake (Figure 22). Andrews Creek originates from Andrews Tarn, at the base of Andrews Glacier. For most of the summer, there is surface outflow from Andrews Tarn, but by late summer, the tarn's stage

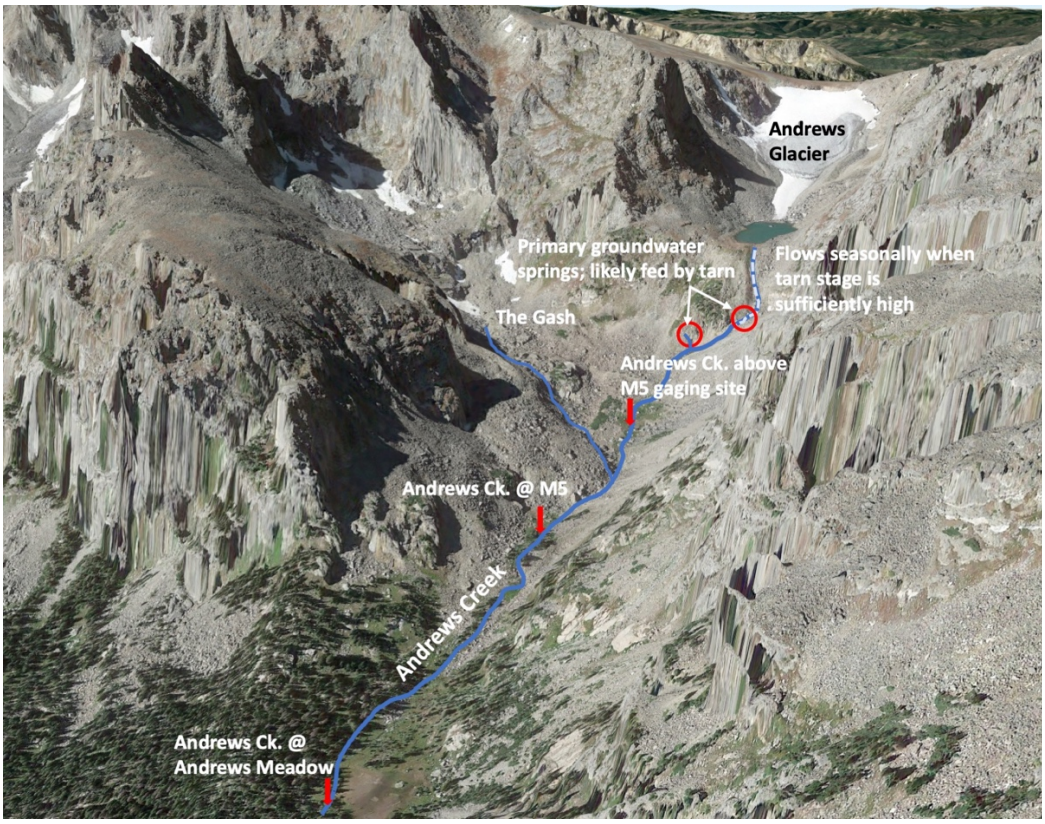

Figure 21. Overview map of Andrews Creek, with stream gaging sites noted.

drops below the outflow elevation. At this time, the creek is fed by groundwater springs that emerge ~100 m downstream of the tarn (locations noted in Figure 21). An additional gaging site was sampled (Andrews Ck above M5) during field campaigns, as this site is above the tributary from the Gash and hence is dominated by meltwater produced by Andrews Glacier.

The Tyndall Creek gage was installed below Emerald Lake, as this was the first suitable channel location downstream of the glacier. Above Emerald Lake, Tyndall Creek is either multi-threaded or flows through talus in the subsurface. The creek is fed by a groundwater spring that emerges ~100 m downstream of Emerald Lake (Figure 22).

Stream stage was measured using TruTrack 1-m capacitance rods, which were typically installed in late June and operated through mid-October. Discharge was measured using salt dilution methodology, where a known mass of NaCl was added to the stream and the conductivity was measured at a distance downstream using a HoBo conductivity data logger. Additionally, colleagues at USGS made three discharge measurements at Andrews Creek in 2016 using the area-velocity method. These discharge measurements were used to build rating curves for each site (Figure 23).

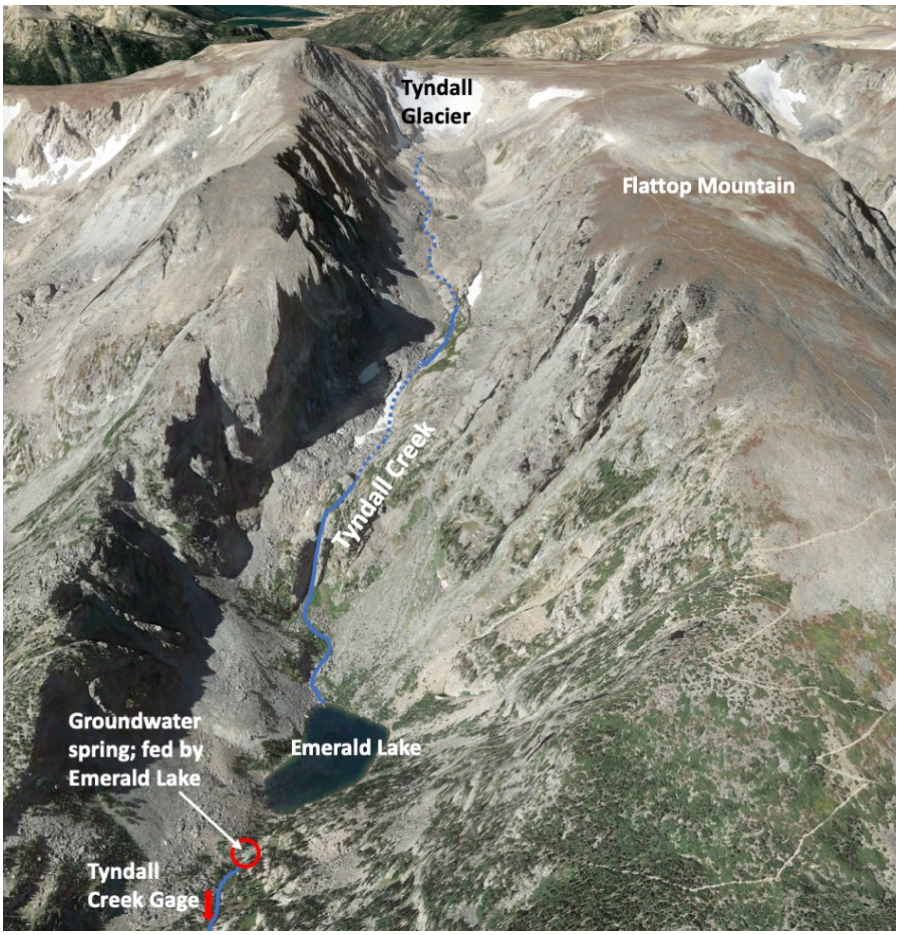

Figure 22. Overview of Tyndall Creek, with stream gaging site noted.

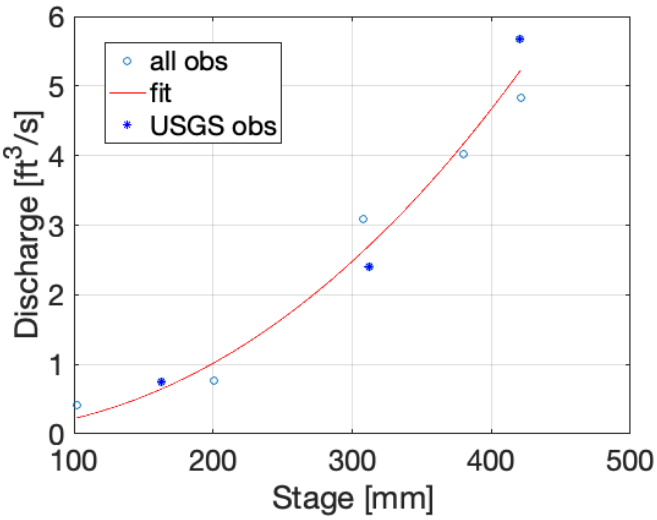

Figure 23. Rating curve for Andrews M5 stream gaging site.

The site specific rating curves were subsequently applied to the stage timeseries to produce a discharge timeseries for both creeks (Figure 24). In all years, the timeseries captures the falling limb of the snowmelt driven hydrograph and both sites had comparable temporal patterns. Andrews Creek exhibited a distinct diel cycle, which lasted until early-mid September, while Tyndall lacked such a cycle since it is primarily groundwater fed.

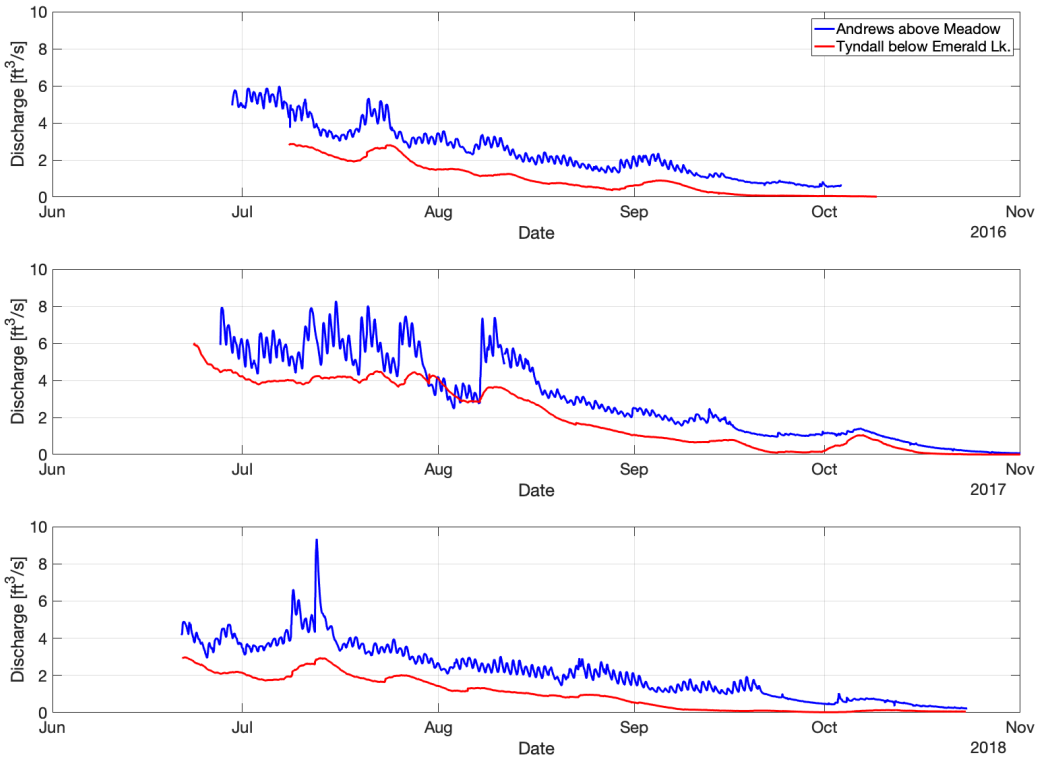

Figure 24. Hydrographs for Andrews (blue) and Tyndall (red) creeks for 2016, 2017, and 2018.

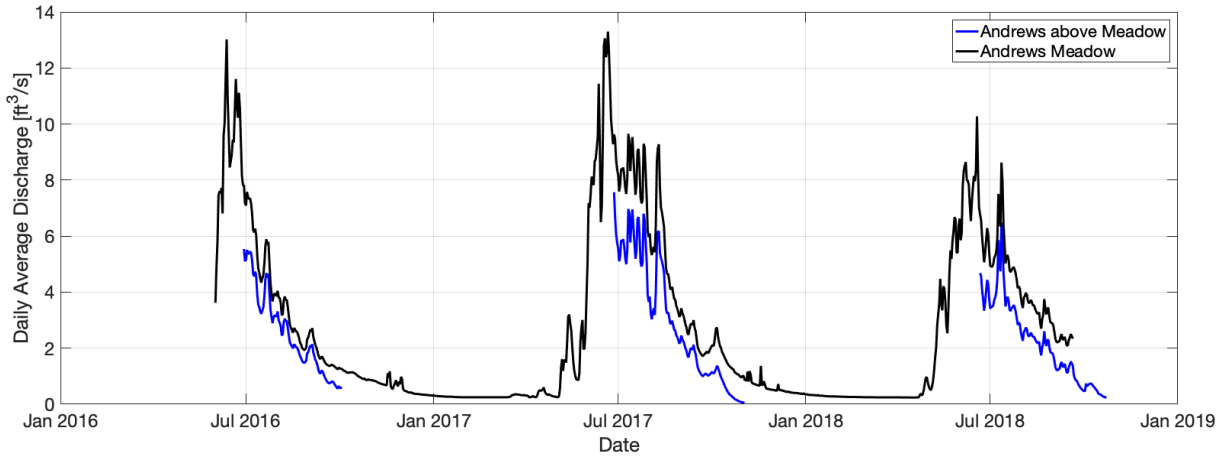

Figure 25. Daily averaged discharge for Andrews Creek at M5 site (blue) and Andrews Meadow (black). Andrews Meadow stream gage is operated by USGS.

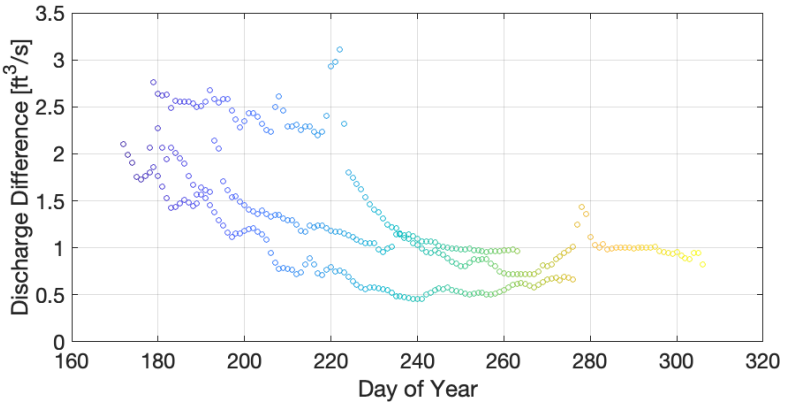

Figure 26. Differences in daily averaged discharge for Andrews Creek M5 and Meadow sites. Differences are colored by the day of year.

As expected, Andrews M5 discharge had less volume but comparable temporal characteristics to Andrews Meadow (Figure 25). The volume differences were between 1.5-2.5 cfs during the primary snowmelt period, but decreased to 0.5-1 cfs after snowmelt ceased (Figure 26). Early seasons differences are attributed to snowmelt between the two sites (~500 m stream length), whereas the late season differences are likely groundwater sourced, as there are no tributaries between the two sites.

A secondary objective of this work was to determine the relative contribution of glacier generated meltwater to the overall discharge of these systems. For this work, we focused on Andrews Creek, and approached the objective with two methods: end-member mixing model/stable isotopes and along-flow discharge sampling. For the former, we collected end-member samples from the tarn, groundwater, precipitation, and snow when in the field, and automatically collected water samples from Andrews Creek every 2-3 days during the summer using an ISCO water sampler. Samples were processed by the University of Wyoming Stable Isotope Facility for δ^2H and $\delta^{18}O$ of water using a Picarro L2130-I Cavity

Ring Down Spectrometer. However, the development of the end-member mixing model was outside the scope of the funded work, but will be pursued in the future.

The second approach involved measuring discharge of Andrews Creek upstream of the M5 site to better isolate stream discharge sourced from Andrews Glacier (Figure 21). On four days during late summer (when glacier melt continued, but snowmelt had declined) in three different years, stream discharge sourced directly from the Andrews Glacier basin accounted for 50-75% of the total discharge at the Andrews M5 site (Table 2).

Table 2. Stream discharge measurements of Andrews Creek.

Date	Andrews M5 discharge [cfs]	Andrews above M5 discharge [cfs]	Percent of Total [%]
9/2/16	0.8	0.5	70
8/11/17	4.8	2.9	59
9/21/17	0.8	0.6	75
8/23/18	3.1	1.5	50

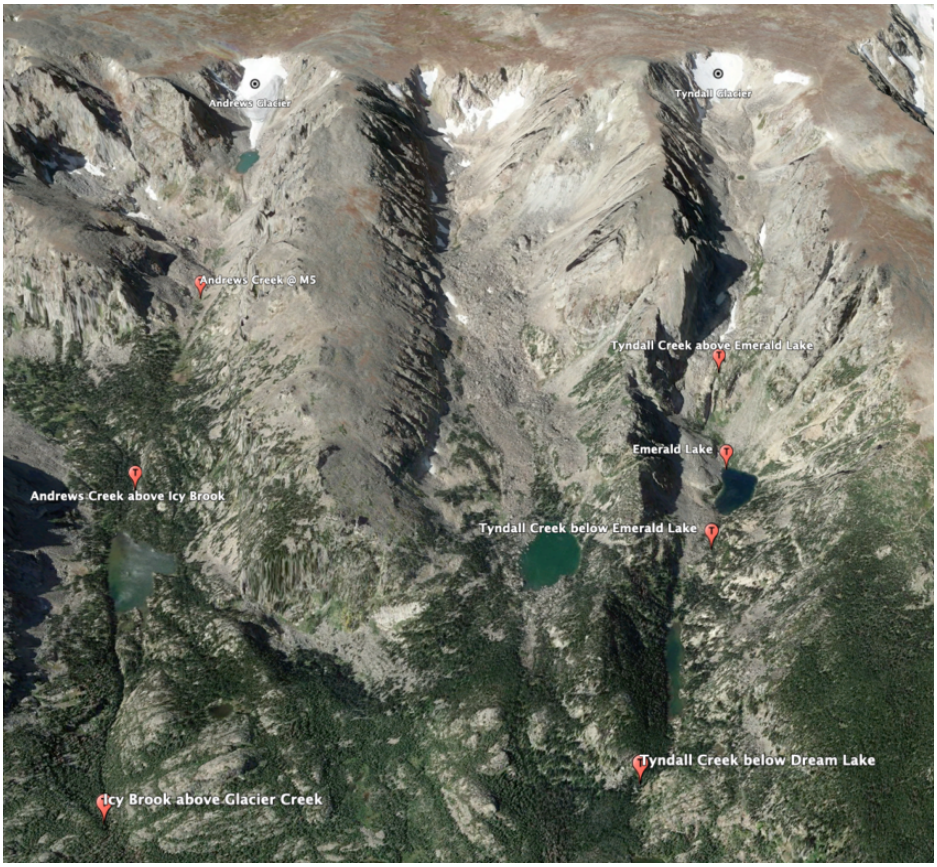

Figure 27. Overview map of stream temperature sensor installations.

In addition to the meltwater volume generated by the glaciers, this water has a distinct thermal signature as it is close to 0 ℃. To quantify this effect, we installed seven stream temperature sensors downstream of the glaciers to measure the spatio-temporal signature of this water (Figure 27). The sensors were installed close to the glacier and at sites further downstream, including above and below Emerald/Dream Lake and the Loch. Stream temperatures closest to the glacier were typically between 1-5 ℃, reached a thermal maxima in late August-early September, and exhibited a clear diel cycle (Figure 28). Both the Loch and Emerald Lake had a significant impact on downstream temperatures, subsequently increasing it by 5℃ or more (Figure 28). Dream Lake resulted in Tyndall Creek warming by another ~3℃.

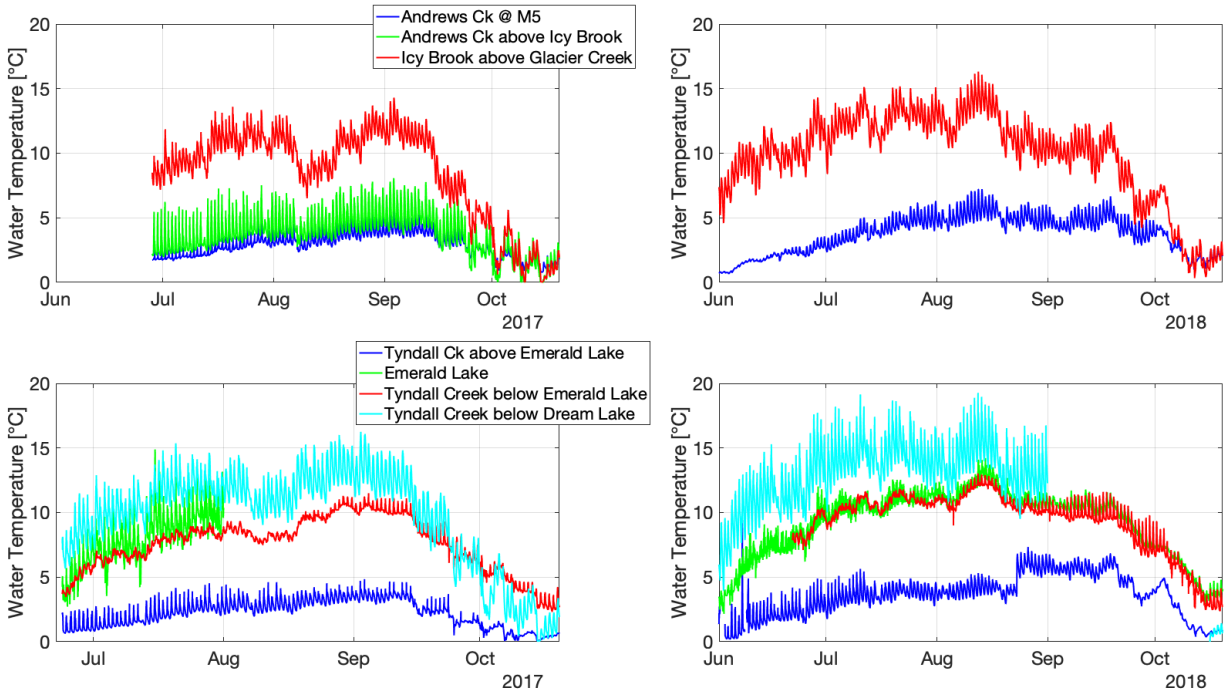

Figure 28. Stream temperatures for Andrews Creek basin (top row) and Tyndall Creek basin (bottom row) in 2017 (first column) and 2018 (second column).

Through an ongoing collaboration with Dr. David Clow and Dr. James Roberts at USGS, we are examining stream temperatures throughout ROMO in order to better quantify the impact of glaciers/perennial ice patches and consider implications for native biota such as Greenback cutthroat trout. More specifically, we've been analyzing stream temperatures for 18 basins nested within nine distinct watersheds. This work has clearly illustrated the strong influence of glacier/ice patches on stream temperatures, with median stream temperatures sourced from glacial meltwater ~2-5℃ colder (Figure 29). We are currently assessing how geologic and vegetation differences between the basins may

influence these signals, in addition to how interannual variability in peak SWE and SWE melt-out date influences stream temperatures (Figure 30).

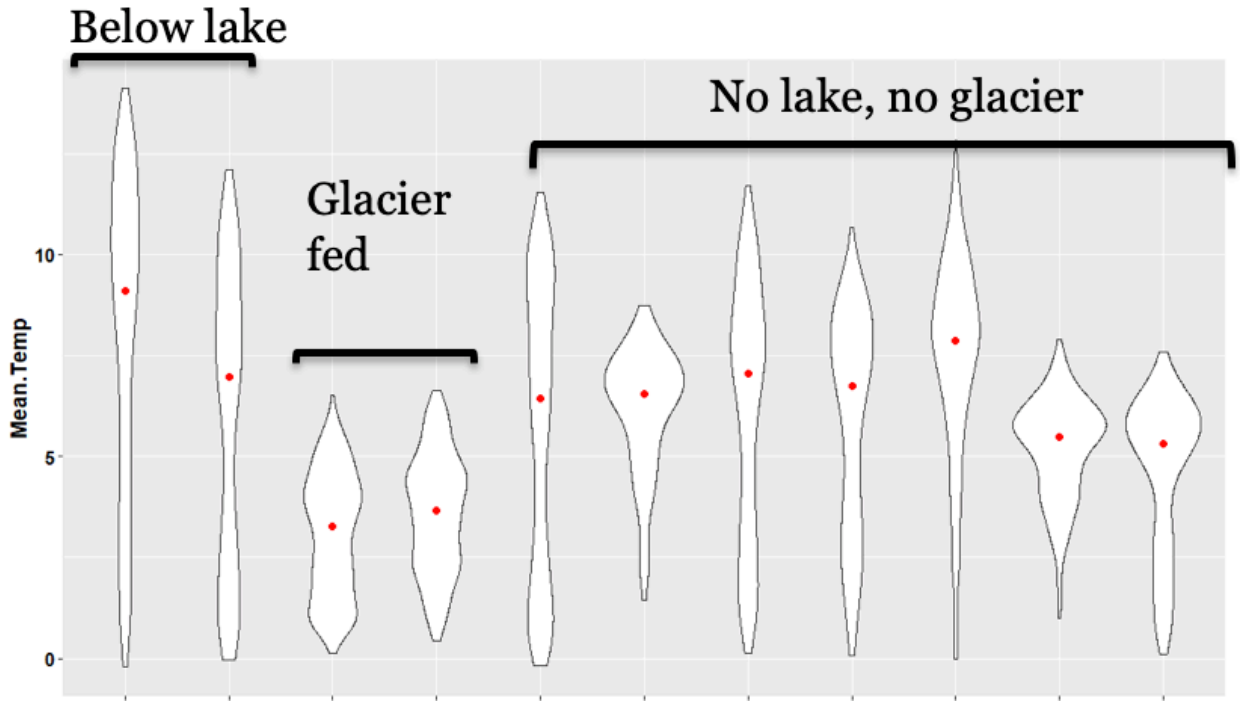

Figure 29. Violin plots of stream temperature for 11 different streams within ROMO.

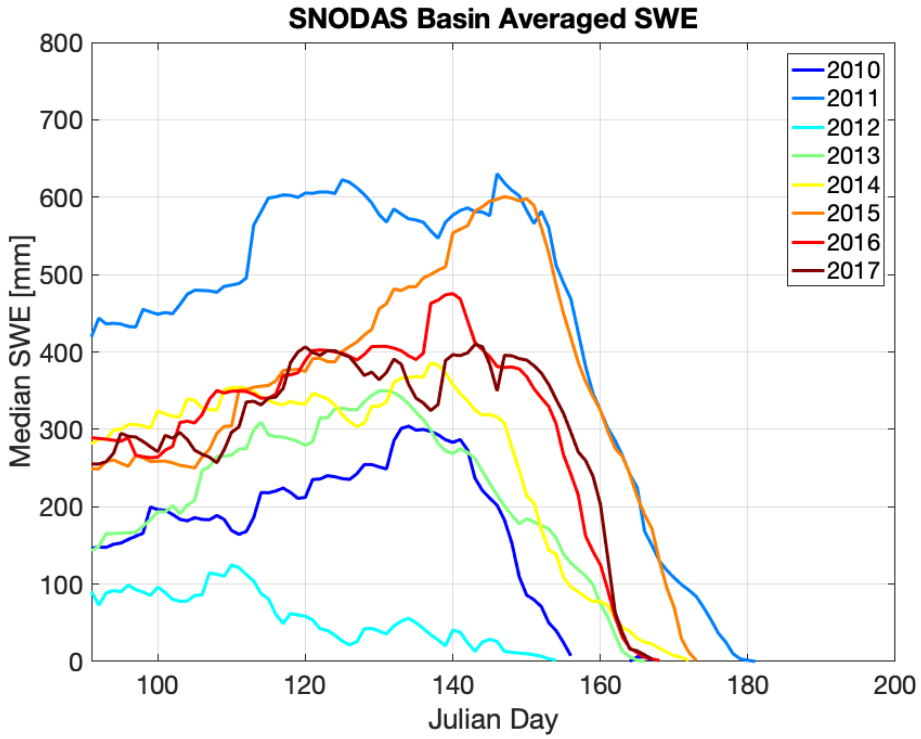

Figure 30. Basin averaged SWE derived from SNODAS for specific watersheds within ROMO between 2010 and 2017.

Section 5. Future Glacier Evolution in ROMO

This project has clearly illustrated the unique topoclimate controls on glacier mass balance in ROMO and more broadly along the Front Range. Additionally, this work has shown that these glaciers supply a significant component of stream discharge in the late summer months, and that this water has a unique thermal signature that may help sustain these alpine ecosystems. The final component of this project focused on trying to better understand how glaciers along CO's Front Range, including ROMO, will change through the end of the century? and secondly, how will future changes in temperature, precipitation timing and precipitation phase modify wind-blown snow redistribution?

To address these research questions, we used SnowModel (Liston and Elder, 2006), a well-validated process-based snow model, in conjunction with NLDAS-2 reanalysis products and assimilated snow water equivalent and wind speed from local SNOTEL/meteorological stations. SnowModel is a spatially distributed physically-based snow evolution modeling system consisting of four sub-models. At present, future climate forcings were derived from downscaled CMIP5 simulations. However, in ongoing work, the model is being forced with high-resolution (4-km) climate change simulations from the Weather Research and Forecasting (WRF) model. These WRF simulations include a historic/control run (Oct. 2000-Sept. 2013) and the second, a CMIP5 ensemble-mean end-of-century high-emissions (RCP 8.5) run.

Preliminary results show mid-century (2045-2055; first row) and end-of-century (2090-2100; second row) change in SWE for April 1, May 1 and June 1 (Figure 31). Mid-century forcings included 1.8

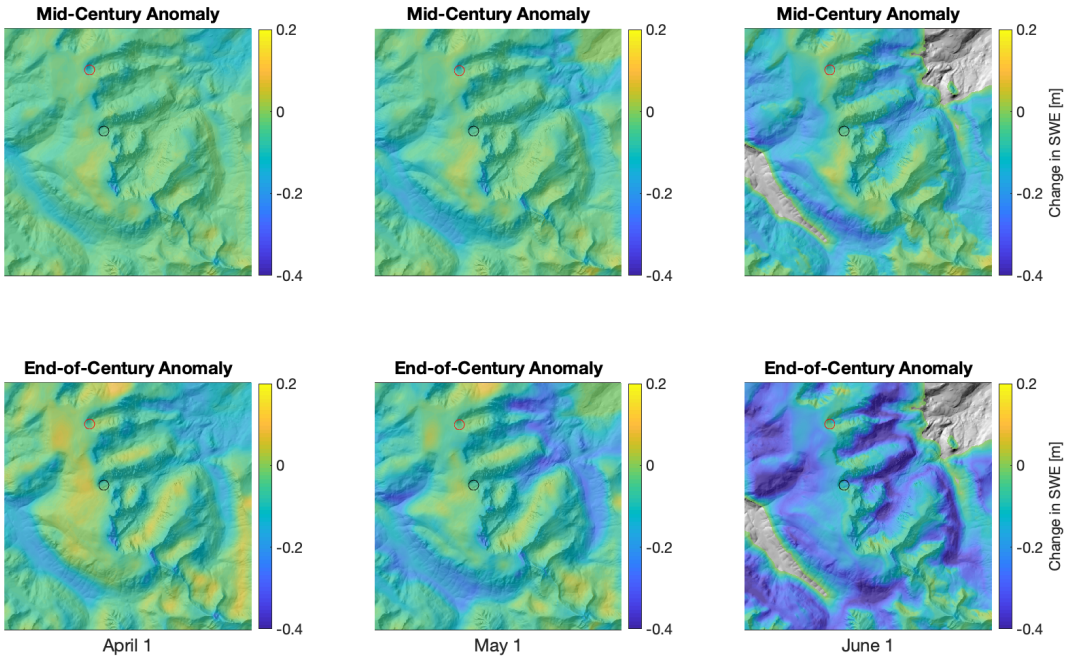

Figure 31. Modeled snow water equivalent anomalies for April 1- June 1 with mid and end-of-century climate forcings.

℃ warming and ~15% precipitation increase, while end-of-century forcings included 4.1 ℃ warming and ~20% precipitation increase. This analysis shows that the highest elevations tend to see no change to a limited increase in SWE for all scenarios except end-of-century June 1. In contrast, low elevations see significant reductions in SWE, particularly as the melt season progresses and for end-of-century climate forcings. SnowModel, although quite sophisticated, was challenged to reproduce the observed snow distribution patterns on Andrews and Tyndall glaciers, which given the magnitude and relative uniqueness of this redistribution, is not that surprising. Ongoing work with Dr. Glen Liston and Dr. Graham Sexstone seeks to implement new processes in the model to account for this extreme redistribution, which will facilitate a more robust assessment of how future forcings will influence glacier mass balance.

Broader Impacts: Outreach and Press Coverage

- Extensive work with Carissa Turner (CDRLC) and Rachel Ames to revamp the ROMO glacier web page. Aspects of this research project will be added to the revamped website, which is planned to launch in late 2019.
- Conducted interview with Jacy Marmaduke at The Coloradoan that resulted in a front-page article on September 19, 2016. http://www.coloradoan.com/story/news/2016/09/19/rocky-mountain-national-park-glaciers/90495554/
- Gave a research seminar at National Park Service Water Resources Division in Fort Collins, CO on February 8, 2017.
- Conducted an interview with students of Vista High Schools in Aurora, CO for a PBS funded story on science in our national parks.
- Collaborated with Ron Bend at Colorado State University for an episode of Outside Science (inside parks) https://www.nps.gov/nature/osip.htm in September 2017.
- Oral presentation at International Glaciological Society Meeting in Boulder, CO on August 16, 2017. https://www.igsoc.org/symposia/2017/boulder/
- Oral presentation at American Geophysical Union Fall Meeting in Washington, D.C. on December 12, 2018. https://agu.confex.com/agu/fm18/meetingapp.cgi/Paper/386411
- Interview with Vishva Nalamalapu, a NPS Science Communication Assistant at the Continental Divide Research and Learning Center (CDRLC) at ROMO, on glaciers in ROMO. June, 2019.
- Invited Talk: Saturday Night in Park presentation at Kawuneeche Visitor Center, ROMO. August, 2019.
- Consulted with Reba McCracken and Simeon Caskey (Grand Teton National Park) on glacier mass balance observations.

Data Access

Airborne NAIP imagery is publicly available at USGS's Earth Explorer: https://earthexplorer.usgs.gov/

USGS 1/3 arc-second DEM is publicly available at USGS's National Map:

https://viewer.nationalmap.gov/basic/

Raw LiDAR point clouds are publicly available in the UNAVCO archive: https://tls.unavco.org/projects/U-056/.
Glacier areas, ground-penetrating radar derived snow and ice thicknesses, LiDAR-derived DEMs, stream temperatures and discharges, and historical repeat photographs are all publicly available here: http://dx.doi.org/10.25675/10217/195598.

Forthcoming Peer-reviewed Publications

At present, three publications are currently in preparation for submission.

1. McGrath, D., M. Willis, B. Hodge, and S. Fassnacht. Topoclimate controls on mass balance sensitivity for very small glaciers along Colorado's Front Range, *Geophysical Research Letters*, in preparation.

2. Roberts, J., D. McGrath, and D. Clow. Examining the role of small glaciers and interannual seasonal snow variability on alpine stream temperatures, Rocky Mountain National Park, CO, *Global Change Biology*, in preparation.

3. McGrath, D., G. Sexstone and G. Liston. Assessing the impact of future climate forcings on the mass balance of very small glaciers. *The Cryosphere*, in preparation.

Acknowledgments

Many individuals helped extensively in the field with data collection, in particular:
Dominick Schneider, Spencer Niebuhr, Brendan Hodge, Michael Fend, Billy Armstrong, Rick Aster, Adam Baxter, Andy Bliss, Alex Brooks, Kevin Bruins, Dave Clow, Tim Covino, Sarah Derego Clark, Matt Hoffman, Matt Kennedy, John Knowles, Paul McLaughlin, Jay Merrill, Allen Pope, Patrick Rizzo, Jessica Stanley, Ryan Webb, Tristan Weiss, Jim Westfall, and Mike Wyatt.

Thank you to Graham Sexstone for collaborating on the SnowModel work, Dave Clow and James Roberts for collaborating on the stream temperature work, and Mike Willis for collaborating on the geodetic mass balance work. Thank you to Steven Fassnacht for helping with project development and the snowpack/temperature analysis, and to Matt Hoffman for sharing the original glacier outlines. Thank you to Noah Molotch for allowing the use of his Mala ProEx GPR unit and Ted Scambos/Rob Bauer for the 250 MHz antenna.

References

Anesio, A.M. and J. Laybourn-Parry, 2012, Glaciers and ice sheets as a biome, *Trends in Ecology and Evolution*, **27**, 219–225.

Baron, J., T. Schmidt and M.D. Hartman, 2009, Climate-induced changes in high-elevation stream nitrate dynamics, *Global Change Biology*, **15**(7), 1777-1789.

Bliss, A., R. Hock, and V. Radić, 2014, Global response of glacier runoff to twenty-first century climate change, *Journal of Geophysical Research Earth Surf*ace, **119**, 717–730, doi:10.1002/2013JF002931.

Edmunds, J., G. Tootle, G. Kerr, R. Sivanpillai, and L. Pochop, 2012, Glacier variability (1967-2006) in the Teton Range, Wyoming, United States, *Journal of American Water Resources Association*, **48**(1), 187-196.

Fassnacht, S., N. Venable, D. McGrath, and G. Patterson, 2018, Sub-seasonal snowpack trends in the Rocky Mountain National Park area, Colorado, USA, *Water*, **10**(562), doi:10.3390/w10050562.

Fountain A.G. and W.V. Tangborn, 1985, The effect of glaciers on streamflow variations, *Water Resource Research,* **21**, 579–586, doi:10.1029/WR021i004p00579.

Gardner, A.S., and 15 others, 2013, A reconciled estimate of glacier contributions to sea level rise: 2003 to 2009, *Science*, **340**, 852–857, doi:10.1126/science.1234532.

Haugen, B., T. Scambos, W.T. Pfeffer, and R.S. Anderson, 2010, Twentieth-century changes in the thickness and extent of Arapaho Glacier, Front Range, Colorado, *Arctic, Antarctic, and Alpine Research*, **42**(2), 198-209.

Heath, J. and J. Baron, 2014, Climate, not atmospheric deposition, drives the biogeochemical mass-balance of a mountain watershed, *Aquatic Geochemistry*, **20**, 167-181, doi:10.1007/s10498-013-9199-2.

Hoffman, M.J., A.G. Fountain, and J.M. Achuff, 2007, 20^{th}-century variations in area of cirque glaciers and glacierets, Rocky Mountain National Park, Rocky Mountains, Colorado, USA, *Annals of Glaciology*, **46**, 349–354.

Hood, E., T.J. Battin, J. Fellman, S. O'Neel and R.G.M. Spencer, 2015, Storage and release of organic carbon from glaciers and ice sheets, *Nature Geoscience*, doi:10.1038/NGEO2331.

Immerzeel, W.M., F. Pellicciotti, and M.F.P. Bierkens, 2013, Rising river flows throughout twenty-first century in two Himalayan glacierized watersheds, *Nature Geoscience*, **6**, doi:10.1038/NGEO1896.

Jacobsen, D., A.M. Milner, L.E. Brown, and O. Dangles, 2012, Biodiversity under threat in glacier-fed river systems, *Nature Climate Change*, **2**, 361–364, doi:10.1038/nclimate1435

Janke, J., 2007, Colorado Front Range Rock Glaciers: Distribution and Topographic Characteristics, *Arctic, Antarctic, and Alpine Research*, **39**(1), 74–83.

Jansson P., R. Hock, and T. Schneider, 2003, The concept of glacier storage: A review, *Journal of Hydrology*, **282**, 116–129. doi:10.1016/S0022-1694(03)00258-0

Kaser, G., M. Großhauser, and B. Marzeion, 2010, Contribution potential of glaciers to water availability in different climate regimes, *Proceedings of the National Academy of Sciences*, **107**, 20223–20227, doi:10.1073/pnas.1008162107.

KellerLynn, K, 2004, Rocky Mountain National Park Geologic Resource Evaluation Report. Natural Resource Report NPS/NRPC/GRD/NRR—2004/004, National Park Service, Denver, Colorado.

Knowles, N., M. Dettinger and D.R. Cayan, 2006, Trends in snowfall versus rainfall in the Western United States, *Journal of Climate*, **19**, 4545–4559.

Liston, G.E. and K. Elder, 2006, A distributed snow-evolution modeling system (SnowModel), *Journal of Hydrometeorology*, **7**, 1259–1276.

Lliboutry, L., 1965, *Traite de Glaciologie*, Masson, Paris.

Leopold, M., G. Lewis, D. Dethier, N. Caine, and M. Williams, 2015, Cryosphere: ice on Niwot Ridge and in the Green Lakes Valley, Colorado Front Range, *Plant Ecology and Diversity*, doi:10.1080/17550874.2014.992489.

Maloof, A., J. Piburn, G. Tootle, and G. Kerr, 2014, Recent alpine glacier variability: Wind River Range, Wyoming, USA, *Geosciences*, **4**, 191-201, doi:10.3390/geosciences4030191.

Marzeion, B., J.G. Cogley, K. Richter and D. Parkes, 2014, Attribution of global glacier mass loss to anthropogenic and natural causes, *Science*, doi:10.1126/science.1254702.

Moore RD, Fleming SW, Menounos B et al, 2009, Glacier change in western North America: Influences on hydrology, geomorphic hazards and water quality, *Hydrologic Processes*, **23**, 42–61, doi:10.1002/hyp.7162

Mote, P.W., 2006, Climate-driven variability and trends in mountain snowpack in Western North America, *Journal of Climate*, 19, 6209–6220.

Outcalt, S.I. and D.D. MacPhail, 1965, *A survey of Neoglaciation in the Front Range of Colorado*. Boulder, CO, University of Colorado Press.

O'Neel, S. and 12 others, 2014, Icefield-to-Ocean Linkages across the Northern Pacific Coastal Temperate Rainforest Ecosystem, *Bioscience*, **65**, 499–512, doi:10.1093/biosci/biv027.

Reynolds, H.A., 2011, Recent glacier fluctuations in Grand Teton National Park, Wyoming [M.S. Thesis]: Pocatello, Idaho State University, 225 p.

Royer TC, and C.E. Grosch, 2006, Ocean warming and freshening in the northern Gulf of Alaska, *Geophysical Research Letters*, doi:10.1029/2006GL026767

Serrano, E., J. Gonzalez-Trueba, J. Sanjose, and L. Del Rio, 2011, Ice patch origin, Evolution and dynamics in a temperate high mountain environment: the Jou Negro, Picos de Europa (NW Spain), *Geografiska Annaler: Series A*, doi:10.111/j.1468-0459.2011.00006.x.

Stewart, I.T., D.R. Cayan, M.D., Dettinger, 2004, Changes in snowmelt runoff timing in western North America under a 'business as usual' climate change scenario, *Climatic Change*, **62**, 217–232.

van Mantgem, P.J. and 10 others, 2009, Widespread increase of tree mortality rates in the Western United States, *Science*, **323**, 521–523, doi:10.1126/science.1165000.

Zemp, M. and 14 others, 2019, Global glacier mass changes and their contributions to sea-level rise from 1961 to 2016, *Nature*, **568**, 382-386, doi:10.1038/s41586-019-1071-0.

Repeat photographs

Andrews Glacier

Tyndall Glacier

Taylor Glacier

Sprague Glacier